Atmospheric Environment 136 (2016) 1–15

Contents lists available at ScienceDirect

Atmospheric Environment

journal homepage: www.elsevier.com/locate/atmosenv

Relationships linking primary production, sea ice melting, and biogenic aerosol in the Arctic

S. Becagli [a, *], L. Lazzara [b], C. Marchese [c], U. Dayan [d], S.E. Ascanius [e], M. Cacciani [f], L. Caiazzo [a], C. Di Biagio [g, h], T. Di Iorio [g], A. di Sarra [g], P. Eriksen [i], F. Fani [b], F. Giardi [a], D. Meloni [g], G. Muscari [l], G. Pace [g], M. Severi [a], R. Traversi [a], R. Udisti [a]

[a] Department of Chemistry, University of Florence, Via della Lastruccia 3, 50019, Sesto Fiorentino, Florence, Italy
[b] Department of Biology, University of Florence, Via Madonna del piano 6, 50019, Sesto Fiorentino, Florence, Italy
[c] Département de Biologie, Chimie et Géographie, Université du Québec à Rimouski, 300 Allée des Ursulines, Rimouski, Québec, G5L 3A1, Canada
[d] Department of Geography, The Hebrew University of Jerusalem, 91905, Jerusalem, Israel
[e] Danish Meteorological Isntitute, Qaanaaq, Greenland
[f] Physics Department, Sapienza University of Rome, Italy
[g] ENEA, Laboratory for Earth Observations and Analyses, Rome, 00123, Italy
[h] LISA, UMR CNRS 7583, Université Paris Est Créteil et Université Paris Diderot Institut Pierre Simon Laplace Créteil, France
[i] Danish Meteorological Institute, Copenhagen, Denmark
[l] Istituto Nazionale di Geofisica e Vulcanologia, INGV, Rome, 00143, Italy

HIGHLIGHTS

- MSA is measured at Ny Ålesund (78.9°N, 11.9°E) and Thule Air Base (76.5°N, 68.8°W).
- Primary production (PP) is calculated by a bio-optical model in the surrounding seas.
- PP explains about the 30% of MSA variability in both the Arctic sites.
- MSA and sea ice melting are correlated (slope: 39 ng $m^{-3}$of MSA/10^6 km^2).
- MSA and ice free marginal ice zone are correlated (slope: 56 ng $m^{-3}$of MSA/10^6 km^2).

GRAPHICAL ABSTRACT

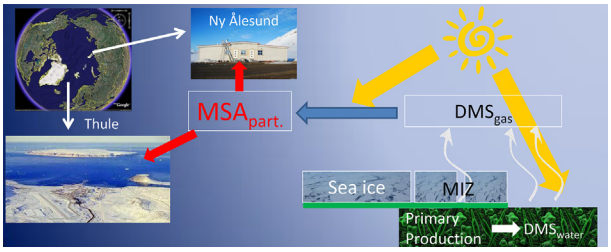

ARTICLE INFO

Article history:
Received 10 November 2015
Received in revised form
1 April 2016
Accepted 4 April 2016
Available online 8 April 2016

Keywords:
MSA
Primary production
Arctic
Marginal sea ice

ABSTRACT

This study examines the relationships linking methanesulfonic acid (MSA, arising from the atmospheric oxidation of the biogenic dimethylsulfide, DMS) in atmospheric aerosol, satellite-derived chlorophyll *a* (Chl-*a*), and oceanic primary production (PP), also as a function of sea ice melting (SIM) and extension of the ice free area in the marginal ice zone (IF-MIZ) in the Arctic. MSA was determined in PM_{10} samples collected over the period 2010–2012 at two Arctic sites, Ny Ålesund (78.9°N, 11.9°E), Svalbard islands, and Thule Air Base (76.5°N, 68.8°W), Greenland. PP is calculated by means of a bio-optical, physiologically based, semi-analytical model in the potential source areas located in the surrounding oceanic regions (Barents and Greenland Seas for Ny Ålesund, and Baffin Bay for Thule). Chl-*a* peaks in May in the Barents sea and in the Baffin Bay, and has maxima in June in the Greenland sea; PP follows the same seasonal pattern of Chl-*a*, although the differences in absolute values of PP in the three seas during the blooms are less marked than for Chl-*a*. MSA shows a better correlation with PP than with Chl-*a*, besides,

* Corresponding author.
E-mail address: silvia.becagli@unifi.it (S. Becagli).

http://dx.doi.org/10.1016/j.atmosenv.2016.04.002

Sea ice melting
Chlorophyll

the source intensity (expressed by PP) is able to explain more than 30% of the MSA variability at the two sites; the other factors explaining the MSA variability are taxonomic differences in the phytoplanktonic assemblages, and transport processes from the DMS source areas to the sampling sites. The taxonomic differences are also evident from the slopes of the correlation plots between MSA and PP: similar slopes (in the range 34.2–36.2 ng $m^{-3}$of MSA/(gC m^{-2} d^{-1})) are found for the correlation between MSA at Ny Ålesund and PP in Barents Sea, and between MSA at Thule and PP in the Baffin Bay; conversely, the slope of the correlation between MSA at Ny Ålesund and PP in the Greenland Sea in summer is smaller (16.7 ng $m^{-3}$of MSA/(gC m^{-2} d^{-1})). This is due to the fact that DMS emission from the Barents Sea and Baffin Bay is mainly related to the MIZ diatoms, which are prolific DMS producers, whereas in the Greenland Sea the DMS peak is related to an offshore pelagic bloom where low-DMS producer species are present. The sea ice dynamic plays a key role in determining MSA concentration in the Arctic, and a good correlation between MSA and SIM (slope = 39 ng m^{-3} of MSA/10^6 km^2 SIM) and between MSA and IF-MIZ (slope = 56 ng m^{-3} of MSA/10^6 km^2 IF-MIZ) is found for the cases attributable to bloomings of diatoms in the MIZ. Such relationships are calculated by combining the data sets from the two sites and suggest that PP is related to sea ice melting and to the extension of marginal sea ice areas, and that these factors are the main drivers for MSA concentrations at the considered Arctic sites.

1. Introduction

Dimethyl sulfide (DMS) produced by marine phytoplankton is the most abundant form of sulfur released from the ocean (Stefels et al., 2007). The precursor of DMS is dimethylsulfoniopropionate (DMSP) which is one of the most relevant phytoplanktonic metabolic compounds, it is mainly produced by Prymnesiophyceae (prymnesiophytes, particularly the coccolithophores *Phaeocystis* spp. and *Emiliania huxleyi*, Keller et al., 1989), Dinophyceae (dinoflagellates, as recently reviewed by Caruana and Malin, 2014), and polar sea-ice diatoms (Kirst et al., 1991; DiTullio et al., 1998). In high-latitude marine areas, DMSP is also produced by sea-ice algae (Levasseur et al., 1994; Arrigo et al., 2012; Boetius et al., 2013) and by the microalgal assemblage in the marginal ice zone (MIZ, the boundary between the open ocean and ice-covered seas Perrette et al., 2011). DMSP is then enzymatically converted into DMS by both microalgae and by heterotrophic bacteria, further it can be uptaken by bacteria and some microalgae (Vila-Costa et al., 2006; Spielmeyer et al., 2011; Ruiz-González et al., 2012), or finally encounter photolysis into other compounds, including MSA. A positive correlation between phytoplankton biomass and DMS, and its derived compound MSA as well (Sharma et al., 2012; Vallina and Simo, 2007), is commonly found: under the so-named 'bloom-dominated regime' DMS conditions (Toole and Siegel, 2004), DMS pattern depends both on microalgal concentration, physiological state and taxonomic composition.

Furthermore, DMS production is related to the physiological state of the cells, increasing under stressed conditions, i.e. stationary/senescent phase (Laroche et al., 1999; Zhuang et al., 2011), grazing (Wolfe and Steinke, 1996), viral lysis (Hill et al., 1998), high UV (which conversely inhibits bacterial DMS uptake; Toole et al., 2006), nutrient-limitation (Sunda et al., 2002) and Fe-limitation (Bucciarelli et al., 2013), named the 'stressed-forced regime' DMS conditions by Toole and Siegel (2004). The 'stressed-forced regime' is typical of temperate seas and the DMS production (and then MSA in atmosphere) are found to be correlated to stress factors such as solar radiation dose, and/or to the specific production index or assimilation number (P^B; i.e. the rate of photosynthetic carbon assimilation per weight of chlorophyll a, Vallina and Simo, 2007; Becagli et al., 2013). Besides, the two DMS regime conditions can co-exist or the latter may follow the "bloom-dominated regime" also in polar sea (Galí and Simó, 2010).

The oceanic DMS flux, estimated using surface ocean DMS concentration data in conjunction with corresponding air-sea exchange coefficients for DMS, has been estimated to be in the range 18–34 Tg yr^{-1} (Lana et al., 2011), accounting for 10–40% of the total sulfur flux (Simó, 2001).

Once in the atmosphere, DMS is oxidized to sulfate and methanesulfonate (MSA) by means of photochemical reactions involving both the heterogeneous and the homogeneous phases (Gondwe et al., 2004). These oxidized sulfur compounds can directly act as cloud condensation nuclei (CCN) or increase the hygroscopicity of already formed particles, enhancing their capability to form CCN (Petters and Kreidenweis, 2007). In this way, the particles formed from DMS oxidation should exert a negative (mitigation) feedback on the solar irradiation - cloud albedo – surface temperature loop at global scale (CLAW hypothesis, Charlson et al., 1987), even though there has been little evidence to support this hypothesis on a regional scale (Quinn and Bates, 2011).

MSA also serves as a tracer for aerosol oceanic sources and changes in MSA may reflect changes in the availability of such sources.

The decline in sea ice extent, coverage and thickness observed in the Arctic over the past decades (e.g., Serreze et al., 2007), and its possible summer disappearance projected within a few decades (Stroeve et al., 2008; Wang and Overland, 2009), is expected to lead to an increase of primary production (PP), both at the local and regional scales (Gradinger, 1995; Loeng et al., 2005; Arrigo et al., 2008; Bélanger et al., 2013). As a consequence of the increased PP the annual DMS flux from the Arctic Ocean is predicted to increase by up to 80% by 2080 (Gabric et al., 2005), possibly as a consequence of changes in phytoplankton productivity associated with shoaling of the mixed layer resulting from sea ice melting.

Several studies have been performed to understand the relation between MSA and the parameters related to biogenic production (Clorophyll-a, hereafter Chl-*a*, sea ice extent) from present day observations and from ice core data in both hemispheres (e.g. Sharma et al., 2012; Isaksson et al., 2005, O'Dwyer et al., 2000; Curran et al., 2003; Abram et al., 2013; Becagli et al., 2009). However, cause and effect associations among, MSA in the atmosphere, changes in sea ice extent, and phytoplankton productivity are yet to be established because several other processes in addition to the source strength play an important role in determining the concentration of MSA at the sampling site. Such processes are the DMS sea-atmosphere exchange, the oxidation efficiency, and the transport processes from the source area to the sampling site (Park et al., 2013; Sharma et al., 2012; Gondwe et al., 2003, 2004).

Moreover, the previous studies do not generally address the role

of primary production, but of some variables which are in some way linked to it, such as Chl-*a* and sea ice.

In this study we combine tree year surface measurements of atmospheric MSA concentration in PM_{10} with measurements of Chl-*a* (by remote sensing ocean color data) and primary production (calculated by a bio-optical, physiologically based, semi-analytical model). PM_{10} measurements are carried out at two Arctic sites: Ny Ålesund (78.9°N, 11.9°E), Svalbard islands, and Thule Air Base (76.5°N, 68.8°W), Greenland. We analyse the relationship between MSA concentration and primary production in the Arctic, focusing on the effects of changes in microalgal assemblages (i.e., taxonomic composition and physiological state) and transport efficiency. Finally, the MSA temporal patterns are compared to the variations in sea ice extent (SIE) and its melting dynamics, aiming to understand the main factors controlling the MSA atmospheric concentrations in the Arctic.

2. Methodology

2.1. Sampling sites

PM_{10} aerosol sampling was performed at the two Arctic sites of Ny Ålesund (Svalbard Island - 78.9°N, 11.9°E) and Thule Air Base (Greenland - 76.5°N 68.8°W). In Fig. 1 the map of the Arctic region is reported, with the sampling locations.

The sampling stations at Ny Ålesund (Gruvebadet station – GVB) and Thule are located few kilometres from the closest villages. Main wind directions indicate that the stations are not influenced by local emissions (Maturilli et al., 2013; Muscari et al., 2014).

By considering a value of 1.8 d^{-1} for the rate of DMS oxidation in the Arctic atmosphere (Lundén et al., 2007) and a typical wind speed for spring-summer month of about 5 m s^{-1} at both sites (Maturilli et al., 2013; Muscari et al., 2014), we defined the three oceanic domains reported in Fig. 1, which may originate the DMS which may be converted into MSA and sampled at Ny Ålesund and Thule.

The cluster analysis performed for the spring-summer seasons of the three years support such finding. In Fig. 2 are reported the cluster analysis of the 4-day wind backtrajectories at 200 m starting at Thule and Ny Ålesund.

The cluster analysis shows that Thule is reached by air masses from the Baffin Bay in 99% of the spring and summer days during the three years. Ny Ålesund has two main source areas: the Barents Sea and the western wind sectors (Greenland Sea). The first one is largely dominant (about 80%) with respect to the second one.

Therefore, Greenland Sea and Barents Sea are expected to be the main source areas for the MSA measured at Ny Ålesund, while Baffin Bay is the source region for MSA at Thule.

The three source regions (encircled areas in Fig. 1) are:

Baffin Bay: 72°N–79°N; 60°W –80°W
Greenland Sea: 73°N–79°N; 10°W–10°E
Barents Sea: 74°N–80°N; 20°E–55°E

Satellite data are retrieved in these areas to estimate primary production to be related with the observations at the two sites.

2.2. Sampling methods and chemical analysis

The aerosol sampling at the two sites was performed by means of a TECORA Skypost sequential sampler equipped with a PM_{10} sampling head operating following the EN 12341 European rules (air flow: 2.3 m^3/h; actual conditions). Aerosol samples were collected on Teflon (PALL Gelman) filters. The sampling started in 2010 at both sites. At Ny Ålesund the sampling is performed only in the period March–September with 24 h resolution, while at Thule the sampling is continuous all year round with 48-h resolution. Some interruptions occurred occasionally at the two sites due to technical problems. Here we report the results of years 2010, 2011 and 2012.

The filters were shipped to Italy, then keep frozen in their plastic Petri dish until they were cut, extracted and analyzed.

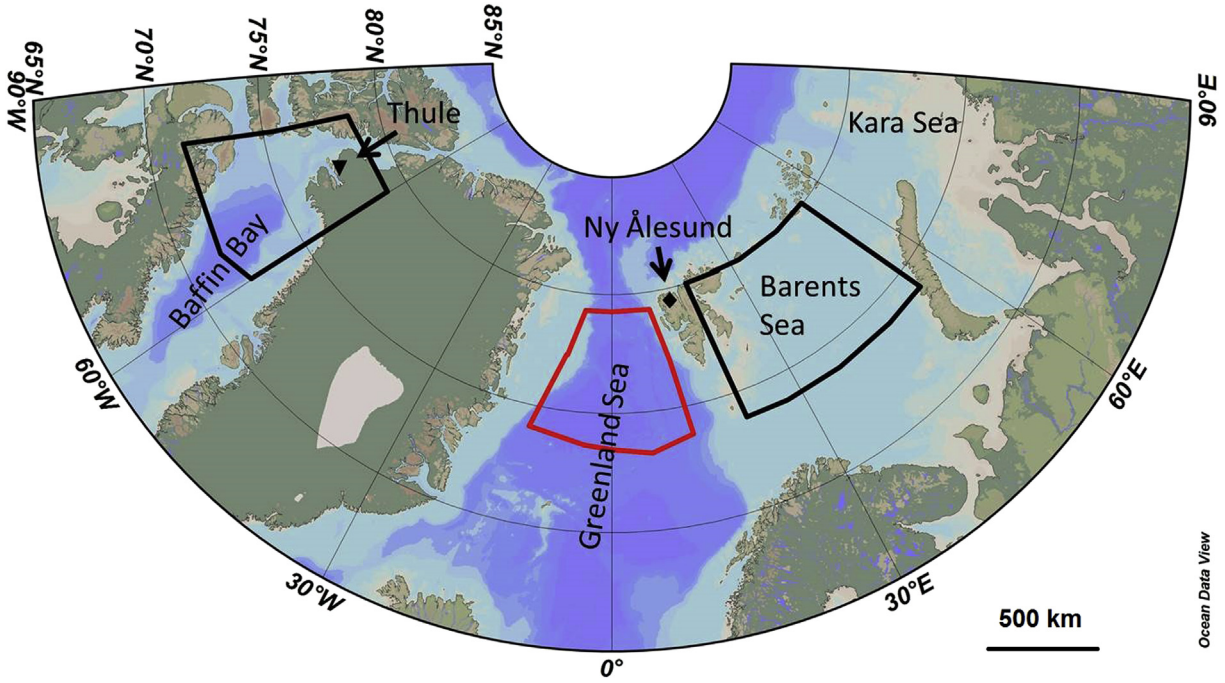

Fig. 1. Bathymetric map of the Arctic region with the sampling sites. The encircled areas are the estimated main source regions for airmasses reaching Thule and Ny Ålesund (see text).

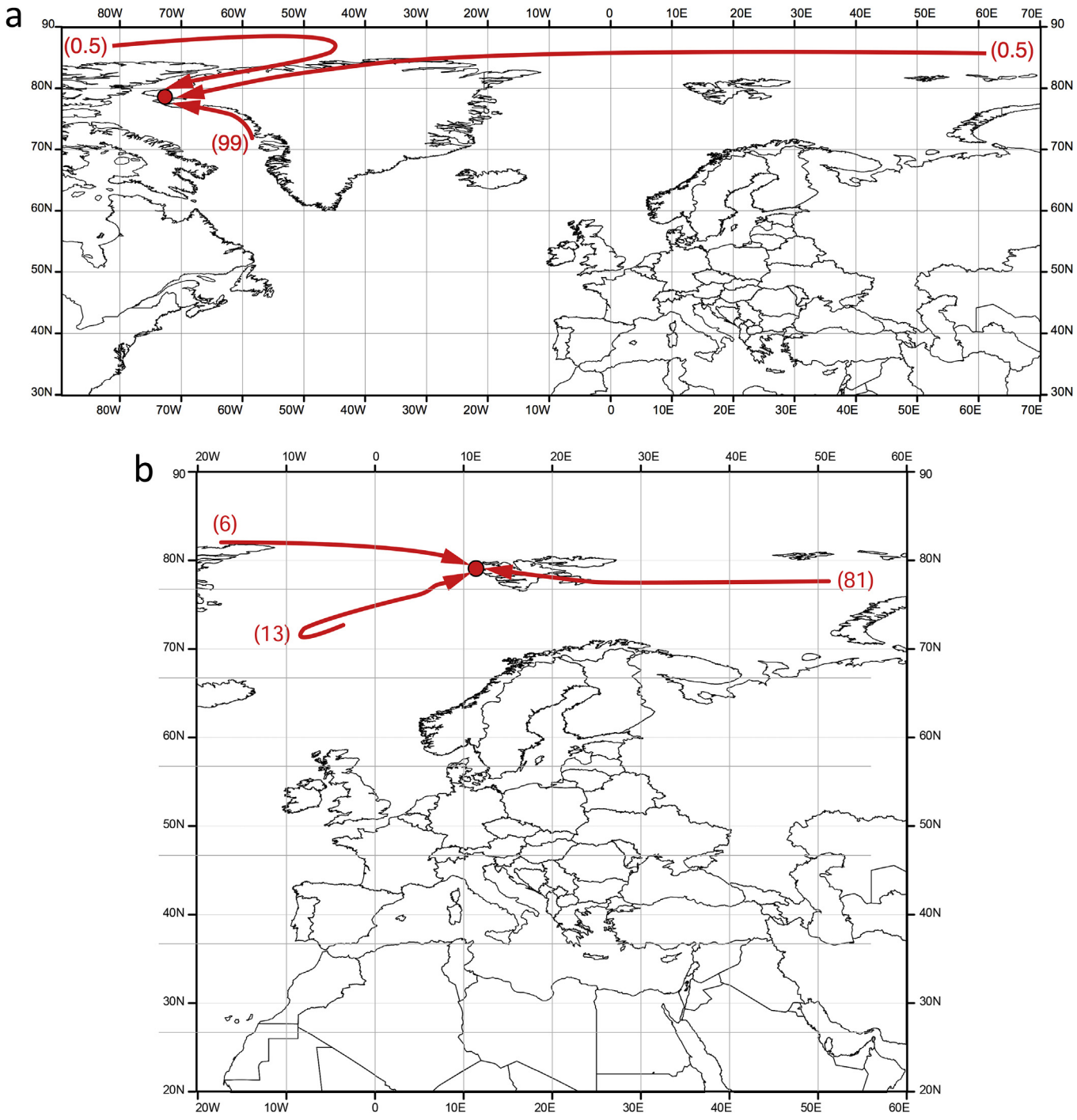

Fig. 2. Air masses origin as indicated by a cluster analysis of the 4-day backtrajectories at 200 m arriving at Thule (a) and Ny Ålesund (b) for spring-summer of years 2010–2012.

Just before the analysis, half of each filter was extracted with 10 mL of ultrapure water (18 MΩ Milli-Q) in ultrasonic bath for 20 min. MSA was determined together with F^- and low molecular weight organic anions by using a Dionex Thermo-Fischer DX600 ion chromatograp equipped with a Thermo-Fischer Dionex AS11 separation column and electrochemical suppression. A Thermo-Fischer Dionex TAC-2 pre-concentration column was used for 1 mL sample injection (Becagli et al., 2011). For MSA, reproducibility on real samples was better than 5%. Filter blank concentrations for MSA were always below the detection limit (0.1 μg L^{-1}, Morganti et al., 2007).

2.3. Satellite data and calculation of primary production

Eight-day averages of chlorophyll *a* concentration, sea surface temperature (SST), and photosynthetically active radiation (PAR) from the Level-3 MODIS-Aqua data sets are obtained from the NASA's Ocean Color website (http://oceancolor.gsfc.nasa.gov/) with a spatial resolution of 9 km, The time series were computed in the three selected domains by spatially averaging the 9 km 8-day datasets. On average, for each year we have more than 50% of valid pixels (Table 1S supplementary meterial). Missing values in Arctic regions are mainly due to either cloudiness or satellite

failure. It should be noted that most of the unavailable data are at the beginning or at the end of the time series. However, overall for both sampling sites there are enough cloud-free data to describe the evolution of Chl-*a*. and PAR.

To estimate the pelagic primary production (PP) within the euphotic layer we used the bio-optical, physiologically-based, and semi-analytical model by Morel (1991). This model, which has been widely validated and extensively used in the Mediterranean Sea (e.g., Marchese et al., 2015; Becagli et al., 2013; Uitz et al., 2012) and globally (e.g., Antoine et al., 1996), combines an atmospheric model (Tanré et al., 1979) with a bio-optical model of light propagation in the water column (Morel, 1988), providing an estimate of photosynthetic irradiance at the sea surface and along the water column. The model takes in to account the parameterization of the main physiological processes of phototrophic growth (Morel, 1991; Morel et al., 1987) and allows the calculation of daily PP, starting from the surface concentration of Chl-*a*. The process of calculating primary production with validation details is described in Lazzara et al. (2010) and Marchese et al. (2015). Overall, in the study areas the pelagic primary production was calculated on a pixel-by-pixel basis starting from Chl-*a*, SST and PAR data, which are the main inputs. Finally, the model uses the General Bathymetric Cart of the Oceans (GEBCO) data to take into account the shallower depth between the entire water column and the euphotic layer, thus significantly reducing PP overestimation in neritic and coastal waters.

The peculiarity of the Arctic Ocean environmental conditions and the behaviour of the primary producers may influence the performance of bio-optical PP models, in several ways and with opposite effects (IOCCG, 2015) depending on the presence of a subsurface chlorophyll maximum, high coloured dissolved organic material (CDOM), sea-ice blooms, cloud cover and specific photosynthesis-irradiance relationship (PE-curves) parameters. However, the performance of this model has been recently tested for net primary production of the entire Arctic Ocean (Lee et al., 2015) in comparison with more than 30 other models, both resolved and integrated for depth or wavelength. The difference between the net primary production estimated by this model and by in situ assessments was within the range 0.54–0.76 (root mean squared deviation) for the tested models, and it was 0.64 for the Morel (1991) model. Hence its general performance in the Arctic Ocean is satisfactory for the purpose of reproducing the PP temporal variability.

Daily sea ice extent (SIE) data were obtained from MASIE-NH (Multisensor Analyzed Sea Ice Extent – Northern Hemisphere) at 4 km of spatial resolution (Meier et al., 2015). MAISE is based on the Interactive Multisensor Snow and Ice Mapping System (IMS) product. MASIE ice extent values were obtained by counting IMS ice-covered cells and multiplying by their area. Sea ice extent is synonymous with sea ice area for this product, but National Snow and Ice Data Center (NSIDC) uses the term extent.

The daily SIE data are averaged on the same time period (8-days) of Chl-a and PP data in order to compare the two data set The 8 day sea ice melting (SIM) was calculated as the difference between two consecutive 8-day average SIE values.

Monthly average sea ice data (extent and area) were obtained by Sea Ice Trends and Climatologies from SMMR and SSM/I-SSMIS, Boulder, Colorado, USA: NASA DAAC at the NSIDC. (Stroeve, 2003).

The monthly sea ice extent was estimated by combining grid cells with sea ice greater than 15% over the considered regions of Baffin Bay, Barents Sea, and Greenland Sea; values less than 15% assumed to be open ocean.

The sea ice extent is different from the sea ice area (SIA) in the monthly data set: the SIA is obtained by summing the concentration of ice within each grid cell over the entire ice expanse.

The marginal ice zone (MIZ) is a boundary between the open ocean and the totally ice-covered ocean, and does not have a unique definition. In previous studies, MIZ has been considered as the region with ice cover less than 40% (Matrai and Vernet, 1997). A more detailed breakdown also has been used, as in Leck and Persson (1996), where the Inner Ice Edge Zone (IIEZ) was defined beetween40 to 80% ice cover. In this study we consider the ice-free surface in the MIZ (IF-MIZ) which is calculate for each month as the difference between sea ice extent and sea ice area. This parameter is related to the MIZ areas where there are favourable conditions for production, and it expresses the surface which is free of ice and where DMS can be transferred from the ocean to the atmosphere. It is known that algal blooms are favored in the MIZ areas (Perrette et al., 2011), where also high water DMS concentrations are measured (Leck and Persson, 1996). These blooms extend several hundred kilometers from the ice edge towards the open ocean (Leck and Persson, 1996; Perrette et al., 2011).

2.4. Trajectories and geopotential height maps

Four-day backward trajectories at 200 m a.s.l were generated using the vertical velocity option of the Hybrid Single-Particle Lagrangian Integrated Trajectory (HYSPLIT) model (Stein et al., 2015). Trajectories were clustered following the method developed by Siebert et al. (2007). The clustering itself was conducted using an algorithm enabling the combination of the 'K-mean' method, which is the most common technique to cluster trajectories and the 'hierarchical' method — the most popular general clustering method (Siebert et al., 2007).

3. Results and discussion

3.1. MSA seasonal evolution

Fig. 3 shows the temporal evolution of MSA in PM_{10} throughout the three years for the two sites. MSA presents the well-known seasonal pattern with increasing concentration in March/April and return to background concentration in September at both sites. The increase in MSA in spring and summer depends on the DMS source (Lana et al., 2011), the photochemical processes and gas to

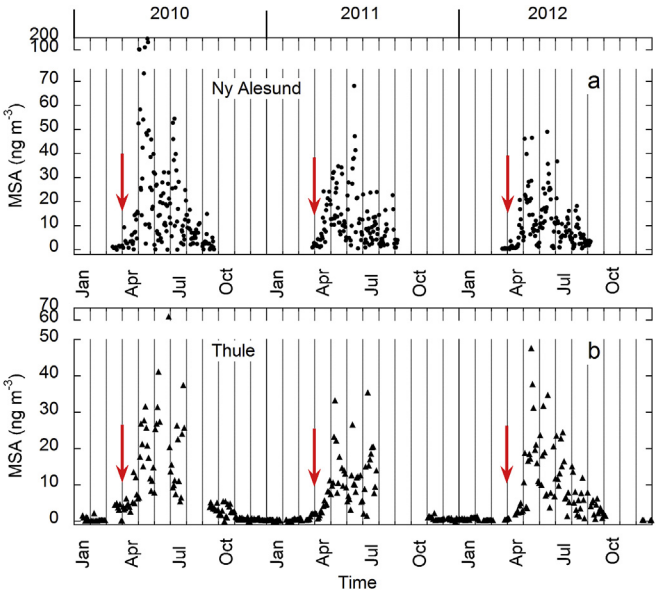

Fig. 3. Time evolution of MSA concentration in PM_{10} measured at the two sampling sites: Ny Ålesund (a) and Thule (b). The arrows indicate the MSA increase at the beginning of April.

Table 1
Average (±1 SD) MSA concentration calculated over the reported years for April–May, June, and July–August periods at Alert, Barrow, Thule and Ny-Ålesund (Zeppelin and Gruvebadet).

	Years	Average MSA ± SD, ng m^{-3}			References
		April–May	June	July–August	
Alert (82°N, 62.3°W, 250 m asl)	1998–2009	12 ± 10	8 ± 6	10 ± 7	Sharma et al., 2012 and references therein
Barrow (71°N, 156.6°W, sea level)	1998–2009	6 ± 8	19 ± 8	20 ± 20	Sharma et al., 2012 and references therein
Ny Alesund -Zeppelin, (78.9°N, 11.9°E, 474 m a.s.l.)	1998–2004	42 ± 33	43 ± 18	42 ± 47	Sharma et al., 2012 and references therein
Ny Alesund -Gruvebadet (78.9°N, 11.9°E, 50 m a.s.l.)	2010–2012	18 ± 27	17 ± 13	10 ± 9	This work
Thule (76.5°N 68.8°W, m asl)	2010–2012	11 ± 10	16 ± 13	13 ± 8	This work

particle conversion producing MSA (in the aerosol) from gaseous DMS (e.g. Karl et al., 2007; Gondwe et al., 2004), and transport in the atmosphere.

In order to compare the MSA values with previous literature data in the Arctic, data were grouped in three periods identified from the characteristics of the MSA seasonal cycle: April–May (generally corresponding to the spring algal bloom at middle and high latitudes), June (transition period), and July–August (summer period, according to Sharma et al., 2012). MSA mean values were calculated over these three periods and reported in Table 1.

The mean MSA concentration shows differences at all sites (Table 1). Seasonal minima are observed in April–May at Barrow (Sharma et al., 2012; Li and Barrie, 1993; Quinn et al., 2007; Maenhaut et al., 1997) and at Thule, and in July–August at Gruvebadet. Very small sprig-summer changes are observed at Alert and Zeppelin. The mean MSA is similar in the Canadian high Arctic at Alert (calculated over the period 1998–2009; Sharma et al., 2012) and at Thule, except in June.

At Ny Ålesund we find larger values with respect to those measured at Thule in April–May, and similar values afterwards. These differences can be attributed to the different timing of sea ice melting, to the distinct features of the microalgal assemblages at the DMS source areas, which in turn are linked to the sea-ice extent, and to the different efficiency of transport processes from the source area to the sampling site.

Differences between Gruvebadet (about 50 m a.s.l.) and the nearby Zeppelin Station (located few hundred meters away, at 470 m a.s.l.), both at Ny Ålesund, deserve more attention. with the mean MSA concentration is about 2.5 times smaller at Gruvebadet than at Zeppelin (Table 1). MSA is affected by the boundary layer dynamics; the gaseous precursor of MSA (DMS) is mixed into the free troposphere during frontal passages and most of the DMS oxidation to MSA occurs in the free troposphere, where the particle surface area is lower and the actinic flux is higher (Bates et al., 1992; Le Quéré and Saltzman, 2009). The vertical stratification reduces MSA transport from the free troposphere to the Arctic boundary layer. Zeppelin site is generally located above the boundary layer in spring and summer, and a MSA concentration higher than at lower altitudes is expected.

3.2. Time series at Ny Ålesund

The seasonal evolution of the 8-day average MSA for the three examined years at Ny Ålesund is reported in Figs. 4 and 6 together with sea ice extent (monthly mean), SST, PAR, Chl-*a* concentration, and PP in the Barents Sea and in the Greenland Sea.

3.2.1. The influence from Barents Sea

In the Barents Sea, Chl-*a* and PP show a sharp maximum in late April or May (depending on the year) when sea ice has just started melting, sea surface temperature was still around 0 °C, and PAR was 50–60% of its seasonal maximum (about 100 W m^{-2} in mid-late June).

These Chl-*a* and PP maxima correspond to the MSA first peak (spring peak - late April or early May depending on the year). Such correspondence is particularly evident (as timing and values trend) in spring 2010. In the following months, Chl-*a* concentration dropped to low values, while PP shows a more gradual decrease, similar to that observed for MSA (Fig. 4).

The high temporal resolution data reported in Fig. 3 show that the MSA concentration at Ny Ålesund begun to increase in April (arrows in Fig. 3). In the Barents Sea, Wassmann et al. (2006a) reported early phytoplankton blooms, starting in April at the MIZ. Such an early bloom was triggered by the stratification induced by the first melting ice and values up to 1.8 gC m^{-2} d^{-1} have been measured in situ, in May, by Matrai et al. (2007). This kind of bloom is usually dominated by the prymnesiophytes (*Phaeocystis pouchetii*, Rat'kova and Wassmann, 2002; Matrai et al., 2007), together with diatoms. Furthermore, high grazing rates were generally found (Wassmann et al., 2006b), which promote high DMS emission. Nevertheless, the blooms are transient local events, due to quick nutrient consumption, and are not propagating as such over the whole region (Perrette et al., 2011). Their transient feature could partially explain the quick drop in Chl-*a* concentrations retrieved by satellite over the Barents Sea (Fig. 4). Moreover, we cannot exclude a relevant contribution to DMSP production by under-ice algae, which always precedes massive DMS release (followed by early and sharp MSA increase) at the beginning of the ice-melting period (as assessed by Asher et al., 2011; for the Antarctic region).

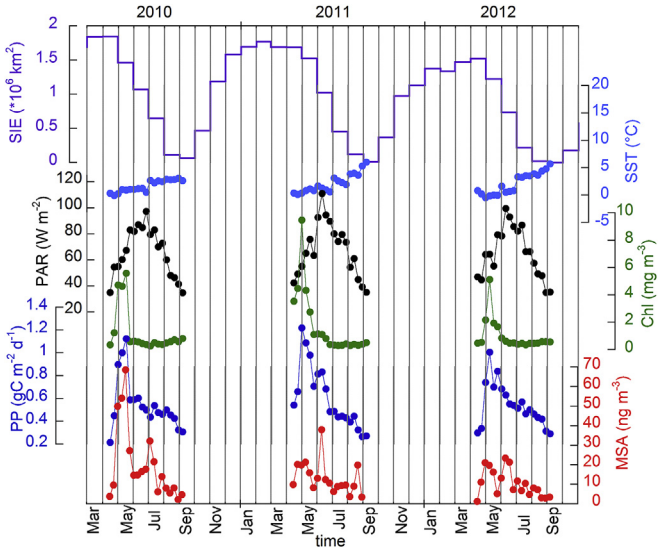

Fig. 4. Three-year evolution of sea ice coverage area (SIE, monthly average), sea surface temperature (SST), photosynthetic active radiation (PAR), Chlorophyll *a* (Chl-*a*), primary production (PP) calculated for the Barents Sea, and MSA at Ny Ålesund. SST, PAR, Chl-a and PP and MSA are calculated as 8-day averages.

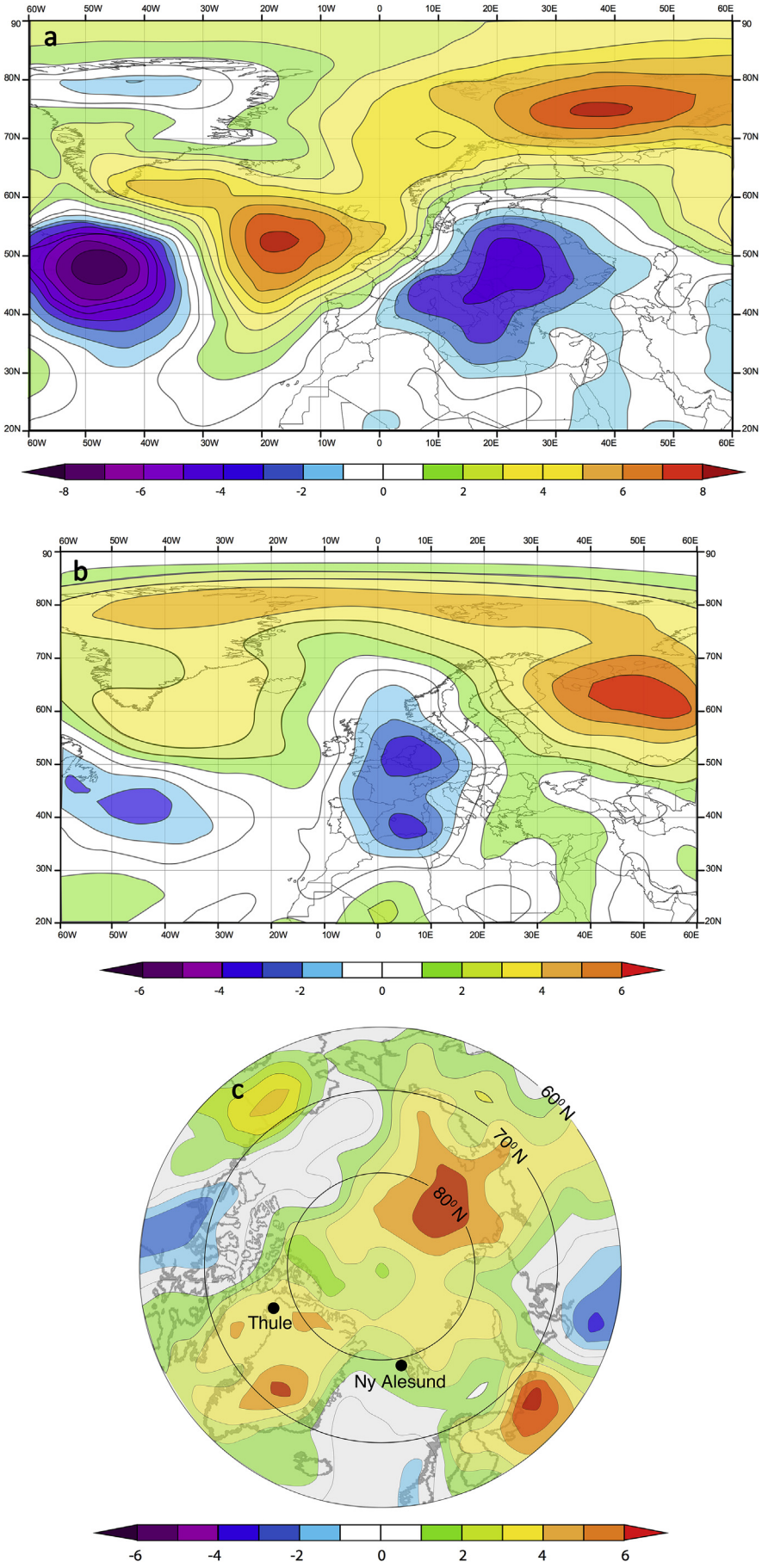

Fig. 5. (a) Sea level pressure composite anomalies and (b) 850 hPa air temperature composite anomaly for the ten days of May 2010 measuring the largest concentration of MSA. (c) Surface temperature anomalies for May 2010 indicating a positive temperature anomaly as compared to 1980–2010 of 2.5–3.5 deg. over most of the regions north of the Arctic circle.

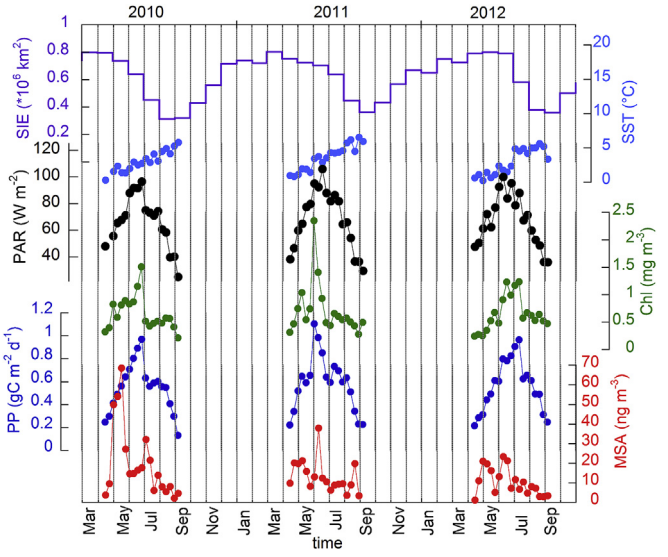

Fig. 6. Three-year evolution of sea ice coverage area (SIE, monthly average), sea surface temperature (SST), photosynthetic active radiation (PAR), Chlorophyll *a* (Chl-*a*), primary production (PP) calculated for the Greenland Sea, and MSA at Ny Ålesund. SST, PAR, Chl-a and PP and MSA are calculated as 8-day averages.

The MSA time series shows a second peak centred in summer (mid-June 2011 and 2012, early-July 2010). This second peak has a correspondence in the PP profile of the Barents Sea only in 2011 and could be related to the Chl-*a* and PP summer peaks in the Greenland Sea (Fig. 6).

When analysing the inter-annual variability of the biomass parameters, some differences in Chl-*a* emerge for the three years. In 2011, the spring values were about twice as much as the ~5 mg m^{-3} observed in 2010 and 2012. The same pattern was observed for PP, even though the differences between 2010, 2012 and 2011 (1.12, 1.01 and 1.22, gC m^{-2} d^{-1}, respectively) were less marked.

3.2.2. The high MSA events in May 2010

The highest MSA concentration, up to 200 ng m^{-3} was measured at Ny Alesund in May 2010. High, but not anomalously high, values of Chl-*a* and PP in the Barents Sea correspond to the MSA peak. A composite synoptic meteo-analysis was performed to understand if these anomalous MSA concentration is related to particular transport processes. Indeed, the sea level pressure composite mean for the selected days in May 2010 (when the ten largest MSA concentration values were measured at Gruvebadet) showed an intense Polar High accompanied by an extension of a Low over Eastern Europe, as confirmed by the composite positive anomaly in sea level pressure (SLP) which exceeded by 5 hPa the long term mean for 1981–2010 (Fig. 5). This relative position of High and Low pressure systems led to a strong SE flow at the surface, advecting warm air from the Siberian Plateau (+6 °C anomaly at the origin) and passing over Barents Sea before reaching Ny Ålesund.

As a result of these frequent easterly winds, May 2010 was characterized by a warming of northern latitudes associated with a cooling of Western Europe. At the 850 mb level (approx. 1.5 km a.s.l.) the air temperature composite anomalies for the extreme MSA days of this particular month at Ny Ålesund were 4 °C above their long term mean values.

This result is consistent with a previous study showing that the largest MSA concentrations at Zeppelin station (Svalbard Island, 450 m a.s.l. near Ny Ålesund) were measured when air masses came from the Barents and Kara Seas (Sharma et al., 2012).

In addition, the May 2010 synoptic configuration led to very different vertical transport regimes. The vertical evolution of the airmasses was studied by calculating 6-day backward trajectories. This analysis shows that, generally, trajectories which originate from the free troposphere, where most of the photochemical processes leading to MSA are expected to take place, are associated with the very high MSA values at Ny Ålesund. Conversely, trajectories confined within the lowest atmospheric layers are obtained on days characterized by minima in MSA. Examples of the trajectory different behaviour on days with very high and low MSA values are shown in Fig. 1S (supplementary material). Thus, a mechanism similar to the one explaining the differences in MSA measurements between Zeppelin and Gruvebadet (see section 3.1) is believed to play an important role in determining the very high MSA values observed at Ny Ålesund.

3.2.3. The influence from Greenland sea

Unlike the Barents Sea, Chl-*a* and PP peak in early summer (June–July) in the Greenland Sea. It should be noticed that the Greenland Sea is more affected by the Gulf Stream than the Barents Sea, and consequently it is free from ice for most of the winter (Gabric et al., 2014), when sea ice is present only in the coastal areas near the Greenland Sea (Pabi et al., 2008). Furthermore, in the Greenland Sea the amplitude of the winter – summer variation in SIE is lower than in the Barents Sea (Figs. 4 and 6). Consequently, the triggering of the microalgal bloom is not strictly dependent on the beginning of sea ice melting, but it could be linked to the maximum light conditions promoting the pelagic bloom, which occurred about one month later than the spring bloom in the Barents Sea.

Moreover, the maximum development of recurrent coccolithophore (*Phaeocystis pouchetii*) and flagellates (including dinoflagellates) blooms takes place in June–July (Scarratt et al., 2007; Lasternas and Agustí, 2010; Gabric et al., 2014) in the northern part of the Greenland Sea (i.e., North of 70°N), thus confirming Chl-*a* and PP patterns with a summer peak. Notably, Chl-*a* concentrations in the Greenland Sea were lower than in the Barents Sea, due to the highly hydrodynamic features of these waters (see Wassmann et al., 2006a, and references therein), confirming the previous results summarized by Sakshaug (2004). Conversely, PP maximum values were of the same order of magnitude in the two considered seas. The same PP values measured in the Greenland and Barents Seas, corresponding to different Chl-*a* values, can be explained by the timing of the Chl-*a* peak. In the Greenland Sea, the Chl-*a* maximum occurred in the period of the maximum PAR (about 100 W m^{-2}), whereas in the Barents Sea it occurred in early spring, when PAR was only 50–60 W m^{-2}. Such findings are likely associated with photo-adaptation, which determines variations of Chl-*a* cell content depending on light availability: under conditions of high PAR cells need less Chl-*a*, and vice-versa (Kirk, 1994). For this reasons, Chl-*a* variations are not necessarily coupled to biomass and PP variations.

3.2.4. Correlation between biologic parameters and MSA

The back trajectory cluster analysis and the PP seasonal pattern revealed that the MSA at Ny Ålesund could originate from two different source areas, Barents Sea in spring, and Greenland Sea in summer. Therefore, the study of the relationship between the biomass parameters and MSA concentrations are separately discussed for the two seasons. Fig. 7 shows the scatter plots between MSA and Chl-*a*, PP and P^B, regression lines are reported if significant (at least $p < 0.05$). MSA and PP appear to be significantly correlated in the Barents Sea, both in Apr–May and in Jun–Sept. It is interesting to notice that PP in the Barents Sea explained more than 30% of the MSA variability at Ny Ålesund. This explained variability is the highest we find between oceanic parameters and MSA at Ny Ålesund.

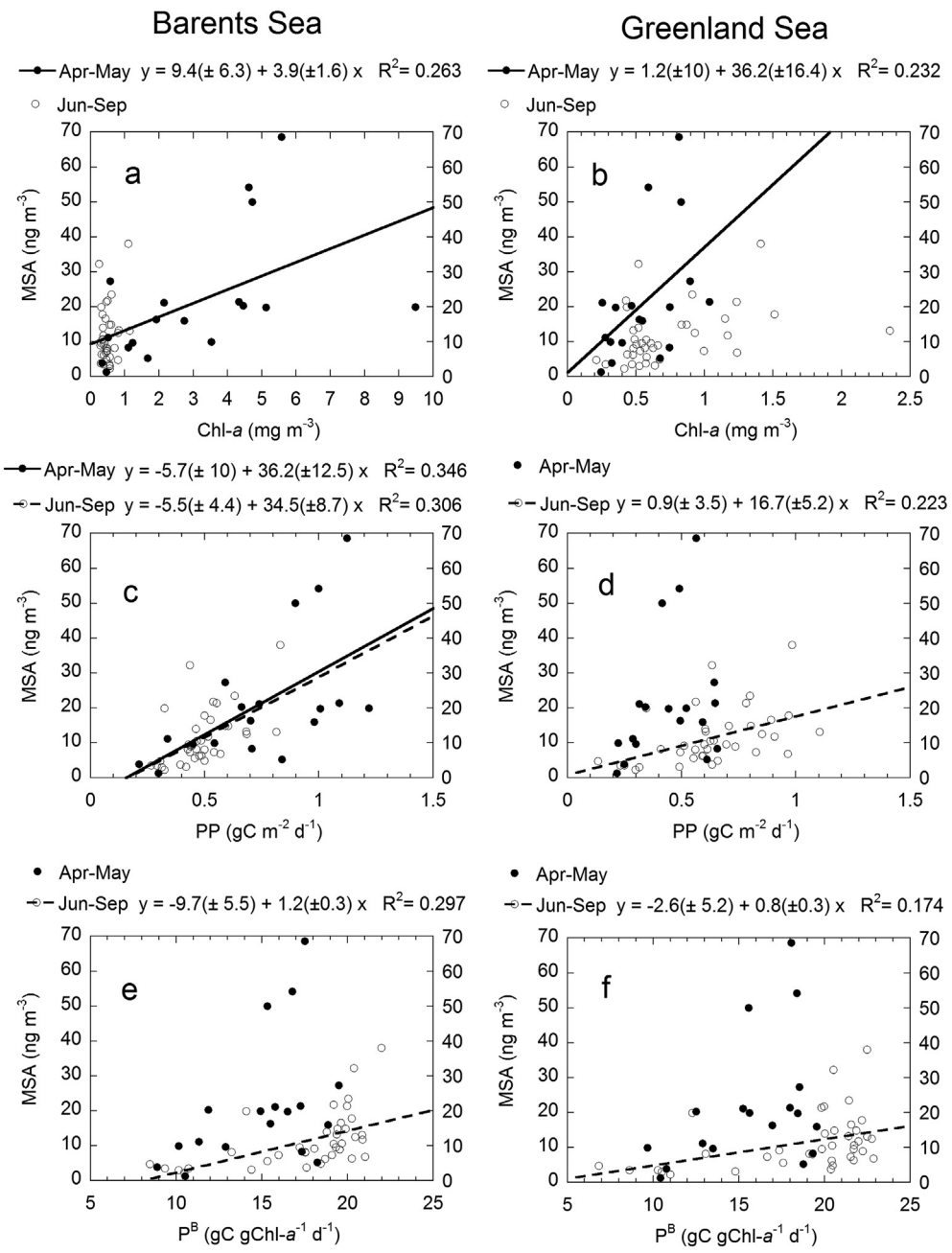

Fig. 7. Scatterplot of MSA at Ny Ålesund and Chl-*a*, PP and P^B for Barents Sea and Greenland Sea in the period April–may (dark dots) and June–September (open circles). Correlation lines are reported if significant at $p < 0.05$ levels.

The correlation between MSA and Chl-*a* in the Barents Sea is statistically significant only in April–May: in a "bloom-dominated regime", as the polar environment is generally assumed to be, the DMS production depends both on PP and biomass concentration. In summer, we observed a significant MSA-PP correlation, while MSA and Chl-*a* were not correlated. This indicates that Chl-*a* and PP are decoupled in summer in the Barents Sea. As previously discussed, photo-adaptation processes can explain this apparent anomaly.

In the Greenland Sea, a significant correlation is found for MSA-Chl-*a* in Apr–May, but such correlation is wrongly forced by the largest values of MSA measured in 2010. Such values should rather be excluded because in this spring the MSA dominant source area is the Barents Sea (section 3.3.2). When ignoring these samples the correlation is no more statistically significant. On the contrary, a good MSA-PP correlation is found in June–September in the Greenland Sea, with an explained variance of about 22%.

The results discussed above show that source intensity (expressed by PP) plays a fundamental role (34% of MSA variability at Ny Ålesund) in controlling the concentration of MSA at Ny Ålesund. The other factors explaining the variability of MSA are: the taxonomic differences in the phytoplanktonic assemblages (see discussion below), transport processes and oxidation pathways and efficiency from DMS to MSA (Le Quéré and Saltzman, 2009; Kerminen and Leck, 2001; Lundén et al., 2007; Gondwe et al., 2003, 2004).

Regarding transport processes, Park et al. (2013) found that hourly to daily variability in the DMS mixing ratios at Zeppelin Station where explained by changes in trajectory, altitude and

speed of air masses overpassing the DMS source prior reaching Svalbard. Is interesting to notice that the time evolution of DMS in spring-summer 2010 reported in Park et al. (2013) for Zeppelin perfectly overlap the MSA temporal evolution measured at Gruvebadet in this study demonstrating that the same factor affect the concentration of MSA and its precursor DMS.

The backward trajectory analysis shows that in April–May 74% (average over the three years) of air masses came from the Barents Sea sector; additionally, the larger the fraction of trajectories originating in the Barents Sea (85.4% in 2010, 75.4% in 2012, 63.8% in 2011), the larger the maximum measured for MSA (192 ng m^{-3} in 2010, 46.5 ng m^{-3} in 2012, and 34.7 ng m^{-3} in 2011).

As previously observed (section 3.3.2), the MSA anomalous high concentrations measured in May 2010 are related to the strong efficiency of transport processes from the Barents Sea. This transport process is related to the meteorological conditions at synoptic scale occurred in the Northern Hemispheric region, which in turn are due to the strong negative phase of the 2010 Arctic Oscillation (Rivière and Drouard, 2015).

The differences in the MSA vs PP slopes between the Barents Sea in spring and the Greenland Sea in summer (36.2 and 16.7 ng $m^{-3}$of MSA/(gC m^{-2} d^{-1}) respectively, Fig. 7) may be attributed to taxonomic differences in the phytoplanktonic assemblages. Indeed, superficial seawater measurements of spring and summer DMS concentrations at the ice edge showed larger values in the Barents Sea than in the Greenland Sea (22 nmol L^{-1} with respect to 10 nmol L^{-1}, Matrai and Vernet, 1997; Galí and Simó, 2010), and were associated with a decaying diatom bloom, found close to the ice pack, and a *Phaeocystis* bloom thriving further offshore (Matrai and Vernet, 1997). Moreover, we have to note that the MIZ microalgae assemblages are prolific producers of DMS and, as previously stated, the MIZ area is largely more relevant for the Barents Sea than for the Greenland Sea.

Finally, it is interesting to notice the significant correlation in the period June–September between MSA and P^B. This suggests the simultaneous presence of a "stress-forced regime" and a "bloom-dominated regime" for the Barents and the Greenland Seas. In a "stress-forced regime", the DMS production reflects also the physiological responses to light and/or nutrient stress by the microalgae that produce DMS, and by the bacteria that produce and consume it. A previous study showed the concurrent presence of these two regimes in the Greenland Sea, i.e., a bloom of *P. puochetii*, together with conditions of DMSP photolysis and bacterial uptake (Galí and Simó, 2010).

3.3. Time series at Thule

Fig. 8 shows the seasonal behaviour of the 8-day average MSA for the three examined years at Thule, together with SST, PAR, Chl-*a* concentration, PP and sea ice extent (monthly average), in the northern part of Baffin Bay. As already reported, 99% of daily backward trajectories in the considered time period arises from this area. As shown in Fig. 8, satellite data of Chl-*a*, SST and PAR are available only starting in late May–June due to the high percentage of cloudy days in April–May over this area.

At Thule, MSA concentration starts increasing in April (arrows in Fig. 3) and a maximum in May is visible in all the considered years. However, a second peak in summer is present only in 2010, when the largest values of MSA were measured (June – Figs. 3 and 8). Consistently, Chl-*a* and PP in the Baffin Bay show large values (about 0.8 gC m^{-2} d^{-1}, Fig. 8) in late May–June in all three years, in correspondence with the largest variations of sea ice coverage.

The annual phytoplankton production was estimated in around 150 gC m^{-2} yr^{-1} for this area (Sakshaug 2004), and diatoms and green flagellates are generally reported as dominant (Bouillon et al., 2002; Vidussi et al., 2004; Luce et al., 2011; Bergeron and Tremblay, 2014), resulting in very low DMSP:Chl ratio. Besides, the release of DMS by copepod grazing played only a minor role (Lee et al., 2003), and the DMS measurements were considerably lower than those predicted by existing models for the distribution of DMS at high latitudes (Kettle et al., 1999).

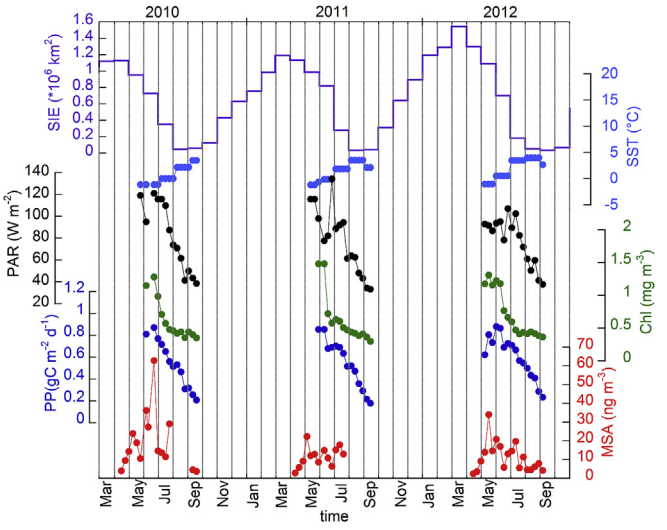

Fig. 8. Three-year evolution of sea ice coverage area (SIE, monthly average), sea surface temperature (SST), photosynthetic active radiation (PAR), Chlorophyll *a* (Chl-*a*), primary production (PP) calculated for the Baffin Bay, and MSA at Thule. SST, PAR, Chl-a and PP and MSA are calculated as 8-day averages.

It has to be considered that the northern part of Baffin Bay is generally occupied by the North Water (NOW) Polynya, a very productive large area sea-ice free in winter and spring. In this area, the phytoplanktonic bloom is favored by the early solar irradiation on the sea-ice free surface seawater and by the upwelling of nutrient-rich water (Stirling, 1981; Smith et al., 1990). In particular, the exposure of surface water to solar radiation much earlier than the adjacent ice-covered waters provides favourable conditions for pelagic primary producers (Tremblay et al., 2002). Several studies demonstrate the strong influence of the phytoplanktonic activity in polynya areas on atmospheric DMS and MSA (e.g. Zhang et al., 2015 and references therein).

The Chl values measured in the upper water column (0–25 m) in a field campaign performed in the NOW Polynya in April–June 1998 (Bouillon et al., 2002) were larger than those obtained in this study, but the seasonal variability was consistent with our data, i.e., low phytoplankton biomass in April and a considerably increase in May and June. In its northern part (i.e., the Smith Sound region) *Phaeocystis* sp., dinoflagellates and other flagellates were dominant in April (Lovejoy et al., 2002), while diatoms appeared later in the study area. Furthermore, the polar under-ice algal communities, whose bloom precedes by two weeks to one month the pelagic one (Guglielmo et al., 2000; Lazzara et al., 2007; Levasseur, 2013), are relevant DMSP producers, as recently highlighted (Arrigo et al., 2012), and can show DMSP:chl ratios significantly higher than the corresponding phytoplanktonic ones (Lee et al., 2001). In this way dinoflagellates and other flagellates, as well as sea-ice algae in the polynya, can be responsible for the increasing MSA concentration at Thule in March and April, when sea ice melting is very low.

Serving as hotspots of both productivity and biodiversity (Marchese, 2015), the NOW polynya constitutes a key habitat for apex predators. The NOW, whose formation is basically due to the appearance of the Smith Sound (~79°N) ice arch that forms

seasonally, begins to expand in March when most areas at the same latitude are still ice-covered. Finally, the NOW reaches its greatest extent in late July when it eventually opens to the bay and stops being a polynya (Tremblay et al., 2002). In particular, the ice bridge represents the northern extent of the polynya and it is essential for the yearly opening of the polynya and its maintenance (Dumont et al., 2009). When this ice bridge fails to consolidate (as recently happened in 2007, 2009 and 2010) the NOW polynya is easily exposed to the passage of large volumes of sea-ice through Nares Strait (Vincent, 2013).

The strong DMS producers usually found at MIZ (see previous citations) and its delayed development could thus explain the special case of the 2010 MSA summer peak (Fig. 8). Furthermore, we can likely suppose that 2010 conditions of extended ice coverage due to the failed polynya formation might have promoted enlarged blooms of sea-ice microalgae, followed by delayed though sudden and thus enhanced release of MSA in the atmosphere, thus contributing to the MSA second peak in summer (late July – Figs. 3 and 8).

3.3.1. *Correlation between biologic parameters and MSA at Thule*

The source area of MSA at Thule is the same for the spring and summer periods, and all data were used together in the correlation analysis. Aside from a few missing data in April, MSA at Thule is significantly correlated with both Chl-*a* and PP and the explained variance of MSA by the two parameter is 27% and 30%, respectively (Fig. 9). Similar percentages were obtained for MSA at Ny Ålesund with respect to Chl-*a* and PP in the Barents Sea. The remaining unexplained variance has to be ascribed to processes related to the atmospheric fate of DMS and not to transport from different source areas, as shown by the trajectory analysis.

The absence of a correlation between MSA and P^B supports the presence of a "bloom dominated regime" in the Baffin Bay.

It is interesting to notice that the slope of the regression line between MSA at Thule and PP in the Baffin Bay (34.2 ± 9.7) is similar to the one found between MSA at Ny Ålesund and PP in the Barents Sea (36.2 ± 12.5 in April–May and 34.5 ± 8.7 in June–September). This suggests that at the same value of PP in the two Seas corresponds the same atmospheric MSA yield. This is mainly due to the similar taxonomic characteristics of the Barents Sea and the Baffin Bay source areas. Indeed, as previous discussed, the main source of MSA is the primary production in the MIZ area present in the two regions.

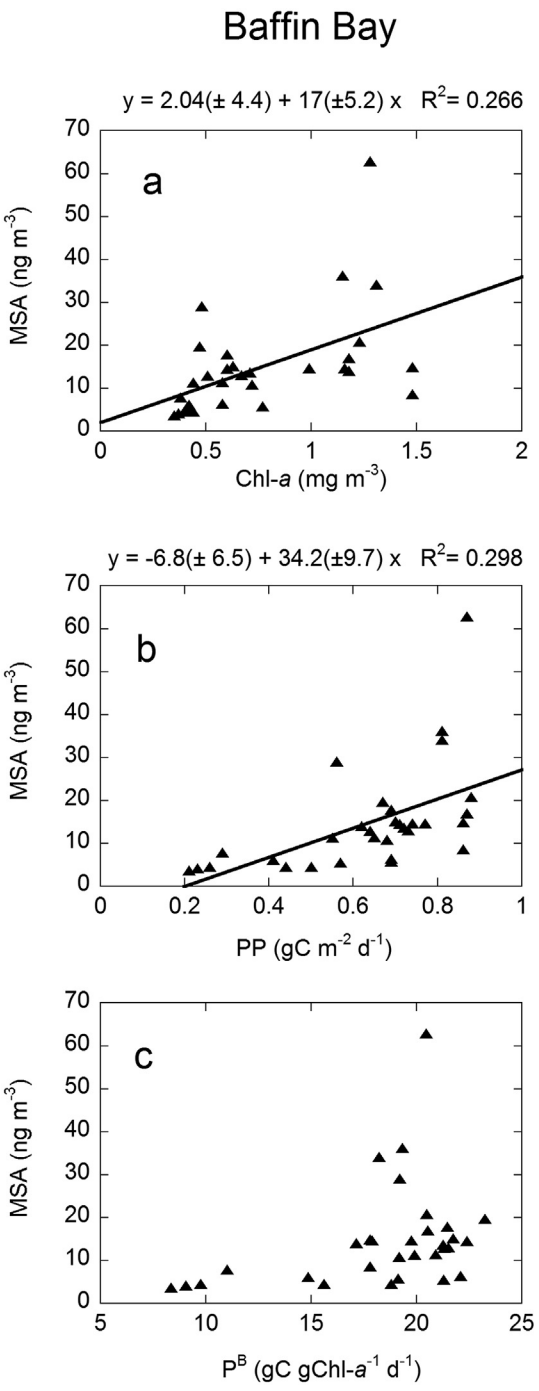

Fig. 9. Scatterplot of MSA at Thule and Chl-*a*, PP and P^B in the Baffin Bay in the period April–May (full circles) and June–September (open circles). Correlation lines are reported if significant at $p < 0.05$ level.

3.4. *Sea ice and MSA*

Sea ice is an important parameter affecting Arctic primary production. It regulates primary production in Arctic shelves by: (i) providing a substrate for algal growth on the underside of the ice (Arrigo et al., 2012); (ii) limiting the photosynthetic radiation available to primary producers; (iii) limiting the development of thermal or fresh water stratification in the freezing season; and (iv) enhancing water stratification during the melting season, therefore regulating the amount of available nutrients in the euphotic layer (Harrison et al., 2013).

The decline in sea ice extent, coverage and thickness observed in the Arctic over the past decades (e.g., Serreze et al., 2007), and its possible summer disappearance within the next few decades (Stroeve et al., 2008; Wang and Overland, 2009), is expected to increase primary production, both at the local and regional scales (Gradinger, 1995; Loeng et al., 2005; Arrigo et al., 2008; Bélanger et al., 2013). The increase in annual primary production has been mainly attributed to a longer phytoplankton growing season (Arrigo et al., 2008).

In previous sections it has been shown the importance of primary production in the MIZ area in Barents Sea and Baffin Bay for determining the MSA atmospheric content at Ny Ålesund and Thule, respectively. In this section we try to correlate two variable related to sea ice dynamic to atmospheric MSA. The two variables are the sea ice melting area (SIM) and ice-free surface in the MIZ (IF-MIZ), which are calculated as reported in section 2.3.

The 8-day average values of MSA at Thule appear to be correlated with SIM areas in Baffin Bay; similarly, MSA at Ny Ålesund appears significantly correlated with the SIM area in the Barents Sea, but not correlated with SIM area in the Greenland Sea (Fig. 10).

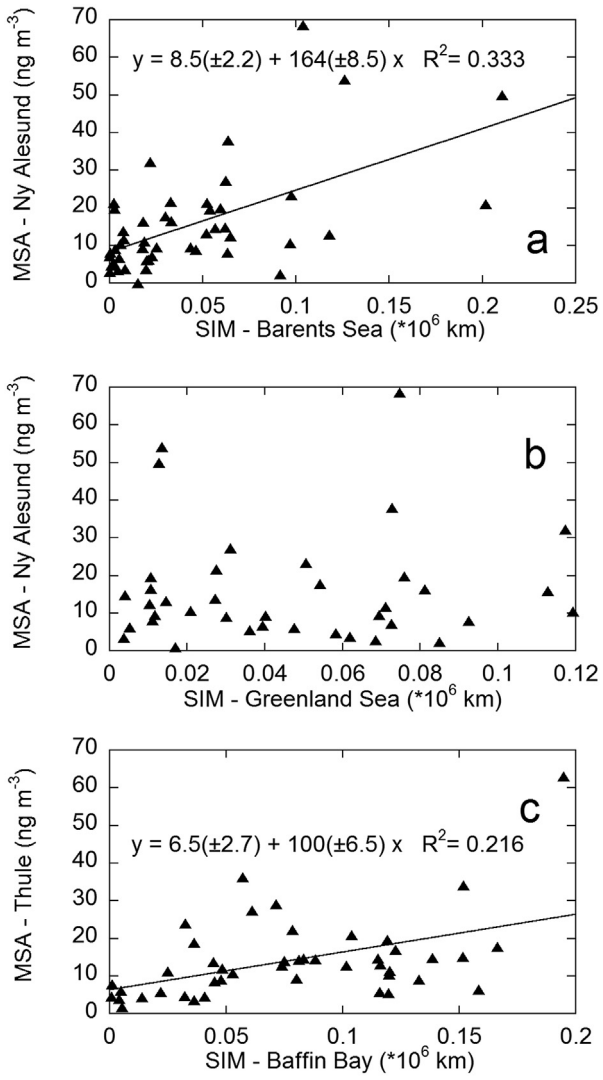

Fig. 10. Scatter plots between 8-day MSA at Ny Ålesund and SIM in (a) the Barents Sea, and (b) the Greenland Sea. c) Scatter plots between 8-day MSA at Thule and SIM in the Baffin Bay. Correlation lines are reported if significant at $p < 0.05$.

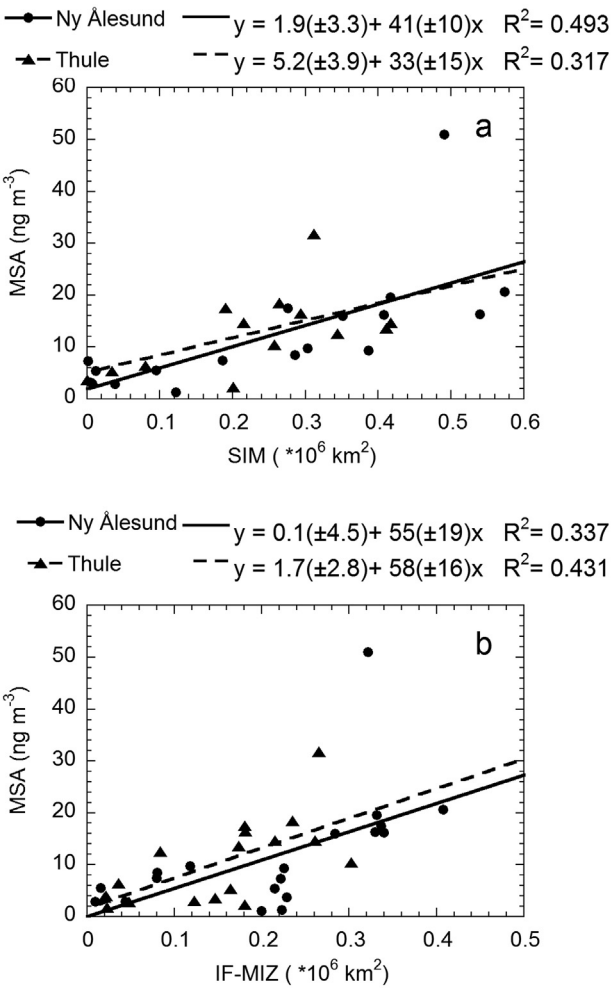

Fig. 11. Correlations between monthly average MSA and (a) monthly average sea ice melting area (SIM) and (b) ice-free marginal ice zone area (IF-MIZ). Dots represent data from Ny Ålesund and Barents Sea, triangles represent data from Thule and Baffin Bay. SIM and IF-MIZ are calculated as reported in section 2.3.

This confirms that the primary production is related to free pelagic blooms and not to MIZ blooms in the Greenland Sea: in this case we do not expect a good correlation between MSA and SIM area, as it is apparent from the data. On the contrary, the correlation between SIM areas and MSA demonstrate the strong influence of the water stratification during the melting season. The stratification regulates the amount of available nutrients in the euphotic layer, thus favouring the bloom in the MIZ area during sea ice melting.

Fig. 11 shows the correlation plots of monthly mean MSA versus SIM and versus IF-MIZ for the cases of primary production in the maginal ice zone (Thule-Baffin Bay, and Ny Ålesund and Bartents Sea). Monthly mean MSA shows a better correlation with SIM with respect to the 8-day average values, and a statistically significant correlation is find between MSA and IF-MIZ. This highlights the importance of the extent of the ice free areas surrounding sea ice in the DMS emission. An increased ice free area leads to more light availability in the euphotic layer, promoting the phytoplankton growth, and to a wider area for sea-air exchange, so enhancing the DMS emission into the atmosphere.

The most important outcome is that almost coincident regression lines are found at the two sites from the monthly mean data, both for MSA versus SIM area and MSA versus IF-MIZ. Therefore, the slopes of the two regression lines calculated on the overall data set, (39 ± 8 and 56 ± 12 ng m^{-3}of MSA/10^6 km^2 respectively), can be considered as a robust estimate of the MSA atmospheric load per million of km^2 of sea ice melted in spring, and the MSA atmospheric load per million of km^2 of ice free area in the MIZ, respectively.

The consistency in the value of the slope may suggest that a robust relationship links MSA and sea-ice melting and MIZ area. A confirmation of this robustness would open the possibility to use MSA in ice-core records to reconstruct the past evolution of sea-ice evolution in the Arctic.

4. Summary and conclusions

This study investigates the relationships among Chl-*a* concentration, PP, P^B and MSA at two Arctic sites, Ny Ålesund, Svalbard islands, and Thule Air Base, Greenland. Three years of data of MSA concentration in the atmospheric particulate sampled at the two sites, satellite-based measurements of Chl-*a* and sea ice distribution, and calculations of primary production at the potential source areas located in the surrounding oceanic regions (Barents and Greenland Seas for Ny Ålesund, and the Baffin Bay for Thule), were used in the analysis. The main findings can be summarized as follows:

- a trajectory analysis was aimed at identifying primary source areas affecting MSA on aerosols sampled at Ny Ålesund and at Thule. The trajectory analysis shows that the MSA measured at Ny Ålesund originates from the Barents Sea and the Greenland Sea, depending on season and on the synoptic meteorological configuration. Virtually all airmass trajectories arriving at Thule come from the Baffin Bay.
- Chl-*a* concentration during the phytoplanktonic bloom shows a large variability in the three considered Arctic Seas, with the largest values measured in the Barents Sea. These values (5–6 times larger compared to the Greenland Sea and Baffin Bay) could be due to the sudden ice-edge bloom occurring in this area in early spring, triggered by the sea ice melting. Conversely, during most of the year the Greenland Sea is not covered by sea ice and offshore *Phaeocystis* sp. blooms are typically recurrent here.
- In the Baffin Bay, the bloom of coccolithophores occurs in early April in the North of the polynya, but the largest DMS production occurs in the MIZ areas in May–June.
- Primary production follows the same seasonal pattern as Chl-*a*, but the differences in PP absolute values in the three seas during the blooms are less marked. This could be due to a photoadaptation process (different amounts of Chl-*a* in the cell as a function of light availability).
- At Ny Ålesund, a significant correlation between MSA and PP in the Barents Sea is found during the spring and summer periods. Conversely, the linear regression MSA – PP in the Greenland Sea is significant only during the summer period. A significant correlation is obtained also between MSA and P^B in the summer period, underlining the concurrent presence of "bloom-dominated regime" and "stress-forced regimes" in both the Barents and Greenland Seas. At Thule, we find a significant correlation between MSA and PP and a poor correlation between MSA and P^B, suggesting a "bloom dominated regime" in the Baffin Bay.
- Source intensity (expressed by PP) is able to explain more than 30% of MSA variability at both sites. The other factors explaining the variability of MSA are the taxonomic differences in the phytoplanktonic assemblages and transport processes from the DMS source areas to the sampling sites.
- Anomalously high values of MSA measured at Ny Ålesund in May 2010 were attributed to a specific synoptic configuration and associated vertical transport, linked to the occurring strong negative phase of the Arctic Oscillation.
- Similar slopes are observed for MSA at Ny Ålesund – PP in the Barents Sea and MSA at Thule – PP in the Baffin Bay correlation plots (in the range 34.2–36.2 ng $m^{-3}$of MSA/(gC m^{-2} d^{-1})); their values are larger than that found for MSA at Ny Ålesund – PP in the Greenland Sea (16.7 ng $m^{-3}$of MSA/(gC m^{-2} d^{-1})). These differences are ascribed to taxonomic differences in the phytoplanktonic assemblages. Indeed, DMS emission in the Barents Sea and in the Baffin Bay is mainly related to the MIZ diatoms that are prolific DMS producers. Conversely, in the Greenland Sea DMS peak is related to an offshore pelagic bloom, resulting in a lower DMS production.
- A significant correlation and a consistent dependency are found between MSA and sea ice melting (slope = 39 ng $m^{-3}$of MSA/10^6 km^2 SIM) and ice free marginal ice zone extension (slope = 56 ng $m^{-3}$of MSA/10^6 km^2 IF-MIZ) (for MSA at Ny Ålesund, with respect to the ice in the Barents Sea; for the MSA at Thule, with respect to the ice in the Baffin Bay). This suggests that the source intensity (i.e., primary production) is related to sea ice melting and to the extension of marginal sea ice areas, and that these factors are the main drivers for MSA concentration in the considered Arctic sites. This is consistent with the general picture which relates emissions in these areas to stress-forced conditions.

The last two points are particularly relevant for understanding the links between climate change and environmental/biological feedbacks. We find that secondary aerosol biogenic production (i.e., MSA) is related to the primary production at the marginal sea ice zone evolution and to the sea ice melting and dynamics during spring and summer rather than to the winter extent of sea ice. Climate variations able to change such dynamics, for instance increasing the melting rate and consequently shortening the melting season, can therefore determine an intense, albeit short in time, phytoplanktonic bloom with a large MSA production. However, how the intensity of such sudden blooms affect the total seasonal primary production and the uptake of CO_2 needs to be further investigated.

Finally, the relationship between MSA and sea-ice melting found in this study opens the possibility to reconstruct the spring/summer sea ice melting and the ice free area in the MIZ evolution in the past from measurements of MSA concentration in ice cores.

Acknowledgements

Measurements at Ny Alesund and Thule were partially supported by projects PRIN 2007 2007L8Y4NB ("Dirigibile Italia") and PRIN 2009 20092C7KRC ("Arctica"), both funded by the Italian Ministry for University and Research (MIUR). Measurements at Thule were also partly supported by the Italian Antarctic Programme, also funded by MIUR, through Projects 2009/A3.04 and 2013/C3.03. This study has been also partially supported by Progetto Premiale ARCA.

The National Aeronautics and Space Administration, Ocean Biology-Distributed Active Archive Center for providing ocean MODIS data is gratefully acknowledged.

The authors gratefully acknowledge the NOAA Air Resources Laboratory (ARL) for the provision of the HYSPLIT transport and dispersion model used in this publication.

Finally, the two anonymous referees are gratefully acknowledge for their constructive suggestions that help in improve the manuscript.

Appendix A. Supplementary data

Supplementary data related to this article can be found at http://dx.doi.org/10.1016/j.atmosenv.2016.04.002.

References

Abram, N.J., Wolff, E.W., Curran, M.A.J., 2013. A review of sea ice proxy information from polar ice cores. Quat. Sci. Rev. http://dx.doi.org/10.1016/j.quascirev.2013.01.011.

Antoine, D., André, J.M., Morel, A., 1996. Oceanic primary production. 2. Estimation at global scale from satellite (coastal zone color scanner) chlorophyll. Glob. Biogeochem. Cycles 10 (1), 57–69.

Arrigo, K.R., Perovich, D.K., Pickart, R.S., Brown, Z.W., van Dijken, G.L., Lowry, K.E., Mills, M.M., Palmer, M.A., Balch, W.M., Bahr, F., Bates, N.R., Benitez-Nelson, C., Bowler, B., Brownlee, E., Ehn, J.K., Frey, K.E., Garley, R., Laney, S.R., Lubelczyk, L., Mathis, J., Matsuoka, A., Mitchell, B.G., Moore, G.W.K., Ortega-Retuerta, E., Pal, S., Polashenski, C.M., Reynolds, R.A., Schieber, B., Sosik, H.M., Stephens, M., Swift, J.H., 2012. Massive phytoplankton blooms under Arctic sea ice. Science 336, 1408.

Arrigo, K.R., van Dijken, G., Pabi, S., 2008. Impact of a shrinking Arctic ice cover on marine primary production. Geophys. Res. Let. 35, L19603. http://dx.doi.org/10.1029/2008GL035028.

Asher, E.C., Dacey, J.W.H., Mills, M.M., Arrigo, K.R., Tortell, P.D., 2011. High concentrations and turnover rates of DMS, DMSP and DMSO in Antarctic sea ice. Geophys. Res. Lett. 38, L23609. http://dx.doi.org/10.1029/2011GL049712.

Bates, T.S., Calhoun, J.A., Quinn, P.K., 1992. Variations in the methanesulphonate to sulfate molar ratio in submicrometer marine aerosol particles over the south Pacific Ocean. J. Geophys. Res. 97 (D9), 9859–9865.

Becagli, S., Castellano, E., Cerri, O., Curran, M., Frezzotti, M., Marino, F., Morganti, A., Proposito, M., Severi, M., Traversi, R., Udisti, R., 2009. Methanesulphonic acid (MSA) stratigraphy from a Talos Dome ice core as a tool in depicting sea ice changes and southern atmospheric circulation over the previous 140 years.

Atmos. Environ. 43, 1051–1058.
Becagli, S., Lazzara, L., Fani, F., Marchese, C., Traversi, R., Severi, M., di Sarra, A., Sferlazzo, D., Piacentino, S., Bommarito, C., Dayan, U., Udisti, R., 2013. Relationship between methanesulfonate (MS^-) in atmospheric particulate and remotely sensed phytoplankton activity in oligo-mesotrophic central Mediterranean Sea. Atmos. Environ. 79, 681–688.
Becagli, S., Ghedini, C., Peeters, S., Rottiers, A., Traversi, R., Udisti, R., Chiari, M., Jalba, A., Despiau, S., Dayan, U., Temara, A., 2011. MBAS (methylene blue active substances) and LAS (linear Alkylbenzene sulphonates) in mediterranean coastal aerosols: sources and transport processes. Atmos. Environ. 45, 6788–6801.
Bélanger, S., Babin, M., Tremblay, J.-É., 2013. Increasing cloudiness in Arctic damps the increase in phytoplankton primary production due to sea ice receding. Biogeosciences 10 (6), 4087–4101. http://dx.doi.org/10.5194/bg-10-4087-2013.
Bergeron, M., Tremblay, J.-É., 2014. Shifts in biological productivity inferred from nutrient drawdown in the southern Beaufort Sea (2003–2011) and northern Baffin Bay (1997–2011). Can. Arct. Lett. 41 (11), 3979–3987.
Boetius, A., Albrecht, S., Bakker, K., Bienhold, C., Felden, J., Fernández-Méndez, M., Hendricks, S., Katlein, C., Lalande, C., Krumpen, T., Nicolaus, M., Peeken, I., Rabe, B., Rogacheva, A., Rybakova, E., Somavilla, R., Wenzhöfer, F., RV Polarstern ARK27-3- Shipboard Science Party7, 2013. Export of algal biomass from the melting Arctic sea ice. Science 339, 1430–1432.
Bouillon, R.–C., Lee, P.A., de Mora, S.J., Levasseur, M., Lovejoy, C., 2002. Vernal distribution of dimethylsulphide, dimethylsulphoniopropionate, and dimethylsulphoxide in the North Water in 1998. Deep Sea Res. II 49, 5171–5189.
Bucciarelli, E., Ridame, C., Sunda, W.G., Dimier-Hugueney, C., Cheize, M., Belviso, S., 2013. Increased intracellular concentrations of DMSP and DMSO in iron-limited oceanic phytoplankton *Thalassiosira oceanica* and *Trichodesmium erythraeum*. Limnol. Oceanogr. 58 (5), 1667–1679.
Caruana, A.M.N., Malin, G., 2014. The variability in DMSP content and DMSP lyase activity in marine dinoflagellates. Prog. Oceanogr. 120, 410–424.
Charlson, R.J., Lovelock, J.E., Andreae, M.O., Warren, S.G., 1987. Oceanic phytoplankton, atmospheric sulphur, cloud albedo and climate. Nature 326, 655–661. http://dx.doi.org/10.1038/326655a0.
Curran, M.A., Palmer, A.S., Van Ommen, T.D., Morgan, V.I., Phillips, K.L., Palmer, A.S., 2003. Ice core evidence for Antarctic sea ice decline since the 1950s. Science 302, 1203–1206.
DiTullio, G.R., Garrison, D.L., Mathot, S., 1998. Dimethylsulfoniopropionate in sea ice algae from the Ross Sea polynya. In: Arrigo, K.R., Lizotte, M.P. (Eds.), Antarctic Sea Ice: Biological Processes, Interactions and Variability. American Geophysical Union, Washington, DC, USA, pp. 139–146.
Dumont, D., Gratton, Y., Arbetter, T.E., 2009. Modeling the dynamics of the north water polynya ice bridge. J. Phys. Oceanogr. 39, 1448–1461. http://dx.doi.org/10.1175/2008jpo3965.1.
Gabric, A.J., Qu, B., Matrai, P.A., Murphya, C., Lu, H., Lin, D.R., Qian, F., Zhao, M., 2014. Investigating the coupling between phytoplankton biomass, aerosol optical depth and sea-ice cover in the Greenland Sea. Dyn. Atmos. Oceans 66, 94–109.
Gabric, A.J., Qu, B., Matrai, P., Hirst, A.C., 2005. The simulated response of dimethylsulfide production in the Arctic Ocean to global warming. Tellus Ser. B 57 (5), 391–403.
Galí, M., Simó, R., 2010. Occurrence and cycling of dimethylated sulfur compounds in the Arctic during summer receding ice edge. Mar. Chem. 122, 105–117.
Gondwe, M., Krol, M., Klaassen, W., Gieskes, W., de Baar, H., 2004. Comparison of modeled versus measured MSA:nss $SO_4^=$ ratios: a global analysis. Glob. Biogeochem. Cycles 18, GB2006. http://dx.doi.org/10.1029/2003GB002144.
Gondwe, M., Krol, M., Gieskes, W., Klaassen, W., de Baar, H., 2003. The contribution of ocean-leaving DMS to the global atmospheric burdens of DMS, MSA, SO_2, and NSS $SO_4^=$. Glob. Biogeochem. Cycles 17 (2), 1056. http://dx.doi.org/10.1029/2002GB001937.
Gradinger, R., 1995. Climate change and biological oceanography of the Arctic Ocean. Philos. Trans. R. Soc. Lond. Ser. A 352, 277–286. http://dx.doi.org/10.1098/rsta.1995.0070.
Guglielmo, L., Carrada, G.C., Catalano, G., Dell'Anno, A., Fabiano, M., Lazzara, L., Mangoni, O., Pusceddu, A., Saggiomo, V., 2000. Structural and functional properties of sea ice communities in the first year sea ice at Terra Nova Bay (Ross Sea, Antarctica). Polar Biol. 23 (2), 137–146.
Harrison, G.W., Børsheim, Y.K., Li, W.K.W., Maillet, G.L., Pepin, P., Sakshaug, E., Skogen, M.D., Yeats, P.A., 2013. Phytoplankton production and growth regulation in the Subarctic North Atlantic: a comparative study of the Labrador Sea-Labrador/Newfoundland shelves and Barents/Norwegian/Greenland seas and shelves. Prog. Oceanogr. 114, 26–45.
Hill, R., White, B., Cottrell, M., Dacey, J.H., 1998. Virus-mediated total release of dimethylsulfoniopropionate, L.: intercomparison of dimethylsulfide oxidation mechanisms for the marine boundary layer: gaseous and particulate sulfur constituents. J. Geophys. Res. 112, D15304. http://dx.doi.org/10.1029/2006JD007, 914,2007.
IOCCG, 2015. Ocean colour remote sensing in Polar Seas. IOCCG Report Series, No. 16. In: Babin, M., Arrigo, K., Bélanger, S., Forget, M.-H. (Eds.), International Ocean Colour Coordinating Group. Dartmouth, Canada.
Isaksson, E., Kekonen, T., Moore, J., Mulvaney, R., 2005. The methanesulfonic acid (MSA) record in a Svalbard ice core. Ann. Glaciol 42, 345–351.
Karl, M., Gross, A., Leck, C., Pirjola, L., 2007. Intercomparison of dimethylsulfide oxidation mechanisms for the marine boundary layer: gaseous and particulate sulfur constituents. J. Geophys. Res 112 (D15304), 914. http://dx.doi.org/10.1029/2006JD007.
Keller, M.D., Bellows, W.K., Guillard, R.R.L., 1989. Dimethylsulfide production in marine phytoplankton. In: Saltzman, E.S., Cooper, W.J. (Eds.), Biogenic Sulphur in the Environment, Am. Chem. Soc. Symp. Ser., vol. 393, pp. 167–182 (Washington, D.C).
Kerminen, V.-M., Leck, C., 2001. Sulfur chemistry over the central Arctic Ocean during the summer: gas-to-particle transformation. J. Geophys. Res. 106 (D23), 32087–32099.
Kettle, A.J., Andreae, M.O., Amouroux, D., Andreae, T.W., Bates, T.S., Berresheim, H., Bingemer, H., Boniforti, R., Curran, M.A.J., DiTullio, G.R., Helas, G., Jones, G.B., Keller, M.D., Kiene, R.P., Leck, C., Levasseur, M., Malin, G., Maspero, M., Matrai, P., McTaggart, A.R., Mihalopoulos, N., Nguyen, B.C., Novo, A., Putaud, J.P., Rapsomanikis, S., Roberts, G., Schebeske, G., Sharma, S., Simó, R., Staubes, R., Turner, S., Uher, G., 1999. A global database of sea surface dimethylsulfide (DMS) measurements and a procedure to predict sea surface DMS as a function of latitude, longitude, and month. Glob. Biogeochem. Cycles 13, 399–444.
Kirk, J.T.O., 1994. Light and Photosynthesis in Aquatic Ecosystems. Cambridge University Press.
Kirst, G.O., Thiel, C., Nothnagel, J., Wanzek, M., Ulmke, R., 1991. Dimethylsulfoniopropionate (DMSP) in ice-algae and its possible biological role. Mar. Chem. 35, 381–388.
Lana, A., Bell, T.G., Simó, R., Vallina, S.M., Ballabrera-Poy, J., Kettle, A.J., Dachs, J., Bopp, L., Saltzman, E.S., Stefels, J., Johnson, J.E., Liss, P.S., 2011. An updated climatology of surface dimethlysulfide concentrations and emission fluxes in the global ocean. Glob. Biogeochem. Cycles 25, GB1004. http://dx.doi.org/10.1029/2010GB003850.
Laroche, D., Vezina, A.F., Levasseur, M., Gosselin, M., Stefels, J., Keller, M.D., Matrai, P.A., Kwint, R.L.J., 1999. DMSP synthesis and exudation in phytoplankton: a modeling approach. Mar. Ecol. Prog. Ser. 180, 37–49.
Lasternas, S., Agustí, S., 2010. Phytoplankton community structure during the record Arctic ice-melting of summer 2007. Polar Biol. 33, 1709–1717. http://dx.doi.org/10.1007/s00300-010-0877-x.
Lazzara, L., Nardello, I., Ermanni, C., Mangoni, O., Saggiomo, V., 2007. Light environment and seasonal dynamics of microalgae in the annual sea ice at Terra Nova Bay (Ross Sea, Antarctica). Antarct. Sci. 19 (1), 83–92. http://dx.doi.org/10.1017/S0954102007000119.
Lazzara, L., Marchese, C., Massi, L., Nuccio, C., Maselli, F., Santini, C., Pieri, M., Sorani, V., 2010. Sub-regional patterns of primary production annual cycle in the Ligurian and North Tyrrhenian seas, from satellite data. Ital. J. Remote Sens. 42 (2), 87e102.
Le Quéré, C., Saltzman, E.S., 2009. Introduction to surface ocean–Lower atmosphere processes. In: Quéré, C.L., Saltzman, E.S. (Eds.), surface ocean-Lower atmosphere processes. American Geophysical Union, Washington, D. C.. http://dx.doi.org/10.1029/2009GM000915
Leck, C., Persson, C., 1996. The central Arctic Ocean as a source of dimethyl sulfide: seasonal variability in relation to biological activity. Tellus Ser. B 48 (2), 156–177. http://dx.doi.org/10.1034/j.1600-0889.1996.t01-1-00003.x.
Lee, P.A., Saunders, P.A., de Mora, S.J., Deibel, D., Levasseur, M., 2003. Influence of copepod grazing on concentrations of dissolved dimethylsulfoxide and related sulphur compounds in the North Water, northern Baffin Bay. Mar. Ecol. Prog. Ser. 255, 235–248.
Lee, P.A., de Mora, S.J., Gosselin, M., Levasseur, M., Bouillon, R.-C., Nozais, C., Michel, C., 2001. Particulate dimethylsulfoxide in Arctic sea-ice algal communities: the cryoprotectant hypothesis revisited. J. Phycol. 37, 488–499. http://dx.doi.org/10.1046/j.1529-8817.2001.037004488.x.
Lee, Y.J., Matrai, P.A., Friedrichs, M., Vincent, M.A., Saba, S., Antoine, D., Ardyna, M., Asanuma, I., Babin, M., Belanger, S., Benoıt-Gagne, M., Devred, E., Fernandez-Mendez, M., Gentili, B., Hirawake, T., Kang, S.-H., Kameda, T., Katlein, C., Lee, S.H., Lee, Z., Melin, F., Scardi, M., Smyth, T.J., Tang, S., Turpie, K.R., Waters, K.J., Westberry, T.K., 2015. An assessment of phytoplankton primary productivity in the Arctic Ocean from satellite ocean color/in situ chlorophyll-a based models. J. Geophys. Res. Oceans 120, 6508–6541. http://dx.doi.org/10.1002/2015JC011018.
Levasseur, M., 2013. Impact of Arctic meltdown on the microbial cycling of sulphur. Nat. Geogr. 6, 691–700. http://dx.doi.org/10.1038/ngeo1910.
Levasseur, M., Gosselin, M., Michaud, S., 1994. A new source of dimethylsulfide (DMS) for the arctic atmosphere: ice diatoms. Mar. Biol. 121 (2), 381–387. http://dx.doi.org/10.1007/BF00346748.
Li, S.-M., Barrie, L.A., 1993. Biogenic sulfur aerosol in the Arctic troposphere: 1. Contributions to total sulfate. J. Geophys. Res. 98, 20,613–20,622. http://dx.doi.org/10.1029/93JD02234.
Loeng, H., Brander, K., Carmack, E., Denisenko, S., Drinkwater, K.F., Hansen, B., Kovacs, K., Livingston, P., McLaughlin, F., Sakshaug, E., 2005. Marine systems. In: Symon, C. (Ed.), Arctic Climate Impact Assesment. Cambridge Univ. Press, New York, pp. 453–538.
Lovejoy, C., Legendre, L., Martineau, M.-J., Bâcle, J., von Quillfeldt, C.H., 2002. Distribution of phytoplankton and other protists in the north water. Deep Sea Res. II 49, 5027–5047.
Luce, M., et al., 2011. Distribution and microbial metabolism of dimethylsulfoniopropionate and dimethylsulfide during the 2007 Arctic ice minimum. J. Geophys. Res. 116, C00G06. http://dx.doi.org/10.1029/2010JC006914.
Lundén, J., Svensson, G., Leck, C., 2007. Influence of meteorological processes on the spatial and temporal variability of atmospheric dimethyl sulfide in the high Arctic summer. J. Geophys. Res. 112, D13308. http://dx.doi.org/10.1029/2006JD008183.
Maenhaut, W., Beyaert, K., Ducastel, G., Havránek, V., Salomonovic, R., Hanssen, J.E.,

1997. Long-term measurements of the atmospheric aerosol composition at Ny Ålesund, Spitsbergen. In: Borrell, P.M., et al. (Eds.), Proceedings of EUROTRAC Symposium '96, vol. 1. Comput. Mech., Southampton, U. K, pp. 273–276.
Marchese, C., Lazzara, L., Peri, M., Massi, L., Nuccio, C., Santini, C., Maselli, F., 2015. Analysis of chlorophyll-a and primary production dynamics in north Tyrrhenian and Ligurian coastal–neritic and ocean waters. J. Coast. Res. 31 (3), 690–701. http://dx.doi.org/10.2112/JCOASTRES-D-13-00210.1.
Marchese, C., 2015. Biodiversity hotspots: a shortcut for a more complicated concept. Glob. Ecol. Conserv. 3, 297–309. http://dx.doi.org/10.1016/j.gecco.2014.12.008.
Matrai, P.A., Vernet, M., 1997. Dynamics of the vernal bloom in the marginal ice zone of the Barents Sea: dimethyl sulfide and dimethylsulfoniopropionate budgets. J. Geophys. Res. 102, 22965–22979.
Matrai, P.A., Vernet, M., Wassmann, P., 2007. Relating temporal and spatial patterns of DMSP in the Barents Sea to phytoplankton biomass and productivity. J. Mar. Syst. 67, 83–101.
Maturilli, M., Herber, A., König-Langlo, G., 2013. Climatology and time series of surface meteorology in Ny-Ålesund, Svalbard. Earth Syst. Sci. Data 5, 155–163. http://dx.doi.org/10.5194/essd-5-155-2013. www.earth-syst-sci-data.net/5/155/2013/.
Meier, W.N., Fetterer, F., Scott Stewart, J., Helfrich, S., 2015. How do sea-ice concentrations from operational data compare with passive microwave estimates? Implications for improved model evaluations and forecasting. Ann. Glaciol. 56 (69), 332–340 doi:3189/2015AoG69A694.
Morel, A., 1988. Optical modelling of the upper ocean in relation to its biogenous matter content (case I waters). J. Geophys. Res. 93 (C9), 10,749–10,768.
Morel, A., 1991. Light and marine photosynthesis: a spectral model with geochemical and climatological implications. Prog. Oceanogr. 26, 263–306.
Morel, A., Lazzara, L., Gostan, J., 1987. Growth rate and quantum yield time response for a diatom to changing irradiances (energy and color). Limnol. Oceanogr. 32 (5), 1066–1084.
Morganti, A., Becagli, S., Castellano, E., Severi, M., Traversi, R., Udisti, R., 2007. An improved flow analysis-ion chromatography method for determination of cationic and anionic species at trace levels in Antarctic ice cores. Anal. Chim. Acta 603, 190–198.
Muscari, G., Di Biagio, C., di Sarra, A., Cacciani, M., Ascanius, S.E., Bertagnolio, P.P., Cesaroni, C., de Zafra, R.L., Eriksen, P., Fiocco, G., Fiorucci, I., Fuà, D., 2014. Observations of surface radiation and stratospheric processes at Thule Air Base, Greenland, during the IPY. Ann. Geophys. 57 (SS0323), 1–14.
O'Dwyer, J., Isaksson, E., Vinje, T., Jauhiainen, T., Moore, J., Pohjola, V., Vaikmäe, R., van de Wal, R.S.W., 2000. Methansulfonic acid in a Svalbard ice core as an indicator of ocean climate. Geophys. Res. Lett. 27 (8), 1159–1162.
Pabi, S., van Dijken, G.L., Arrigo, K.R., 2008. Primary production in the Arctic Ocean, 1998–2006. J. Geophys. Res. 113, C08005. http://dx.doi.org/10.1029/2007JC004578.
Park, K.-T., Lee, K., Yoon, Y.-J., Lee, H.-W., Kim, H.-C., Lee, B.-Y., Hermansen, O., Kim, T.-W., Holmén, K., 2013. Linking atmospheric dimethyl sulfide and the Arctic Ocean spring bloom. Geophys. Res. Lett. 40, 155–160. http://dx.doi.org/10.1029/2012GL054560.
Perrette, M., Yool, A., Quartly, G.D., Popova, E.E., 2011. Near-ubiquity of ice-edge blooms in the Arctic. Biogeosciences 8, 515–524. http://dx.doi.org/10.5194/bg-8-515-2011.
Petters, M.D., Kreidenweis, S.M., 2007. A single parameter representation of hygroscopic growth and cloud condensation nucleus activity. Atmos. Chem. Phys. 7, 1961–1971. http://dx.doi.org/10.5194/acp-7-1961-2007.
Quinn, P.K., Shaw, G., Andrews, E., Dutton, E.G., Ruoho-Airola, T., Gong, S.L., 2007. Arctic haze: current trends and knowledge gaps. Tellus Ser. B 59, 99–114.
Quinn, P.K., Bates, T.S., 2011. The case against climate regulation via oceanic phytoplankton sulphur emissions. Nature 480, 51–56. http://dx.doi.org/10.1038/nature10580.
Rat'kova, T.N., Wassmann, P., 2002. Seasonal variation and spatial distribution of phyto- and protozooplankton in the central Barents Sea. J. Mar. Syst. 38 (1–2), 47–75.
Rivière, G., Drouard, M., 2015. Understanding the contrasting north Atlantic oscillation anomalies of the winters of 2010 and 2014. Geophys. Res. Lett. 42, 6868–6875. http://dx.doi.org/10.1002/2015GL065493.
Ruiz-González, C., Galí, M., Sintes, E., Herndl, G.J., Gasol, J.M., Simó, R., 2012. Sunlight effects on the osmotrophic uptake of DMSP sulphur and leucine by polar phytoplankton. PLoS One 7 (9), e45545. http://dx.doi.org/10.1371/journal.pone.0045545.
Sakshaug, E., 2004. Primary and secondary production in the Arctic seas. In: Stein, R., MacDonald, R.W. (Eds.), The Organic Carbon Cycle in the Arctic Ocean. Springer, pp. 57–81 (Chapter 3).
Scarratt, M.G., Levasseur, M., Michaud, S., Roy, S., 2007. DMSP and DMS in the Northwest Atlantic: late-summer distributions, production rates and sea-air fluxes. Aquat. Sci. 69, 292–304.
Serreze, M.C., Holland, M.M., Stroeve, J., 2007. Perspectives on the Arctic's shrinking sea-ice cover. Science 315 (5818), 1533–1536. http://dx.doi.org/10.1126/science.1139426.
Sharma, S., Chan, E., Ishizawa, M., Toom-Sauntry, D., Gong, S.L., Li, S.M.D., Tarasick, W., Leaitch, W.R., Norman, A., Quinn, P.K., Bates, T.S., Levasseur, M., Barrie, L.A., Maenhaut, W., 2012. Influence of transport and ocean ice extent on biogenic aerosol sulfur in the Arctic atmosphere. J. Geophys. Res. 117, D12209. http://dx.doi.org/10.1029/2011JD017074.
Siebert, P., Frank, A., Formayer, H., 2007. Synoptic and regional patterns of heavy precipitation events in Austria. Theor. Appl. Climatol. 87, 139–153.
Simó, R., 2001. Production of atmospheric sulfur by oceanic plankton: biogeochemical, ecological and evolutionary links. Trends Ecol. Evol. 16 (6), 287–294. http://dx.doi.org/10.1016/S0169-5347(01)02152-8.
Smith, S.D., Muench, R.D., Pease, C.H., 1990. Polynyas and leads: an overview of physical processes and environment. J. Geophys. Res. 95, 9461–9479.
Spielmeyer, A., Gebser, B., Pohnert, G., 2011. Investigations of the uptake of dimethylsulfoniopropionate by phytoplankton. Chem. BioChem 12, 2276–2279.
Stefels, J., Steinke, M., Turner, S., Malin, G., Belviso, S., 2007. Environmental constraints on the production and removal of the climatically active gas dimethylsulphide (DMS) and implications for ecosystem modeling. Biogeochem 83, 245–275.
Stein, A.F., Draxler, R.R., Rolph, G.D., Stunder, B.J.B., Cohen, M.D., Ngan, F., 2015. NOAA's HYSPLIT atmospheric transport and dispersion modeling system. Bull. Amer. Meteor. Soc. 96, 2059–2077. http://dx.doi.org/10.1175/BAMS-D-14-00110.1.
Stirling, I., 1981. Introduction. In: Stirling, I., Cleator, H. (Eds.), Polynyas in the Canadian Arctic. Canadian Wildlife Service, Ottawa, pp. 5–6. Canadian Wildlife Service Occasional Paper 45.
Stroeve, J., 2003. Sea Ice Trends and Climatologies from SMMR and SSM/I-SSMIS. Sea Ice Extent. NASA DAAC at the National Snow and Ice Data Center, Boulder, Colorado USA. On line at: http://nsidc.org/data/nsidc-0192.html.
Stroeve, J., Serreze, M., Drobot, S., Gearheard, S., Holland, M., Maslanik, J., Meirer, W., Scambos, T., 2008. Arctic Sea ice extent plummets in 2007. Eos Trans. AGU 89 (2), 13. http://dx.doi.org/10.1029/2008EO020001.
Sunda, W., Kleber, D.J., Kiene, R.P., Huntsman, S., 2002. An antioxidant function for DMSP and DMS in marine algae. Nature 418, 317–320.
Tanré, D., Herman, M., Deschaps, P.Y., De Leffe, A., 1979. Atmospheric modelling for space measurements of ground reflectances, including bidirectional properties. Appl. Opt. 18, 3587–3594.
Toole, D.A., Siegel, D.A., 2004. Light-driven cycling of dimethylsulfide (DMS) inthe Sargasso sea: closing the loop. Geophys. Res. Lett. 31, L09308. http://dx.doi.org/10.1029/2004GL019581.
Toole, D.A., Slezak, D., Kiene, R.P., Kieber, D.J., Siegel, D.A., 2006. Effects of solar radiation on dimethylsulfide cycling in the western Atlantic Ocean. Deep Sea Res. I 53, 136–153.
Tremblay, J.E., Gratton, Y., Fauchot, J., Price, N.M., 2002. Climatic and oceanic forcing of new, net, and diatom production in the North Water. Deep Sea Res. Part II 49, 4927–4946.
Uitz, J., Stramski, D., Gentili, B., D'Ortenzio, F., Claustre, H., 2012. - Estimates of phytoplankton class-specific and total primary production in the Mediterranean Sea from satellite ocean color observations. Glob. Biogeochem. Cycles 26. http://dx.doi.org/10.1029/2011GB004055.
Vallina, S.M., Simo, R., 2007. Strong relationship between DMS and the solar radiation dose over the global surface ocean. Science 315, 506e508.
Vidussi, F., Roy, S., Lovejoy, C., Gammelgaard, M., Thomsen, H.A., Booth, B., Tremblay, J.-E., Mostajir, B., 2004. Spatial and temporal variability of the phytoplankton community structure in the North Water Polynya, investigated using pigment biomarkers Can. J. Fish. Aquat. Sci. 61, 2038–2052.
Vila-Costa, M., Simo, R., Harada, H., Gasol, J.M., Slezak, D., Kiene, R.P., 2006. Dimethylsulfoniopropionate uptake by marine phytoplankton. Science 314, 652–654.
Vincent, R.F., 2013. The 2009 North Water anomaly. Remote Sens. Lett. 4, 1057–1066. http://dx.doi.org/10.1080/2150704x.2013.837227.
Wang, M., Overland, J.E., 2009. A sea ice-free summer Arctic within 30 years? Geophys. Res. Lett. 36, L07502. http://dx.doi.org/10.1029/2009GL037820.
Wassmann, P., Reigstad, M., Haug, T., Rudels, B., Carroll, M.L., Hop, H., Gabrielsen, W.G., Falk-Petersen, S., Denisenko, S.G., Arashkevich, E., Slagstad, D., Pavlova, O., 2006a. Food webs and carbon flux in the Barents Sea. Prog. Oceanogr. 71, 232–287.
Wassmann, P., Slagstad, D., Wexels Riser, C., Reigstad, M., 2006b. Modelling the ecosystem dynamics of the marginal ice zone and central Barents Sea. II. Carbon flux and interannual variability. J. Mar. Syst. 59, 1–24.
Wolfe, G.V., Steinke, M., 1996. Grazing-activated production of dimethyl sulphide (DMS) by two clones of *Emiliania huxleyi*. Limnol. Oceanogr. 41, 1151–1160.
Zhang, M., Chen, L., Xu, G., Lin, Q., Liang, M., 2015. Linking Phytoplankton Activity in Polynyas and Sulfur Aerosols over Zhongshan Station, East Antarctica. J. Atmos. Sci 72, 4629–4642. http://dx.doi.org/10.1175/JAS-D-15-0094.1.
Zhuang, G., Yang, G., Yu, J., Gao, Y., 2011. Production of DMS and DMSP in different physiological stages and salinity conditions in two marine algae. Chin. J. Oceanogr. Limnol. 29 (2), 369–377.